

# Photovoltaic Cells Based on Organic and Inorganic Thin Films at Research Development Centre for Materials and Electronic and Optoelectronic Devices from University of Bucharest

*Ștefan ANTOHE*

*University of Bucharest, Faculty of Physics, P.O.Box:MG-11, Bucharest-Magurele, 077125 ROMANIA, E-mail: [santohe@solid.fizica.unibuc.ro](mailto:santohe@solid.fizica.unibuc.ro)*

## Abstract

*In this work are summarized the electrical and photoelectrical properties of the organic photovoltaic cells based on the organic thin layers. Starting with the single-layer photovoltaic structures, the ITO/CuPc/Al and ITO/TPyP/Al has been prepared and characterized, where the organic layers of CuPc and TPyP, are Copper Phthalocyanine and 5,10,15,20-Tetra (4-Pyridyl)21H,23H-Porphine, respectively. The photovoltaic structures based on the p-n heterojunction present at the interface between two organic layers, like, ITO/CuPc/TPyP/Al and ITO/Chl a/TPyP/Al, exhibits stronger spectral sensitivity and better spectral matching to a solar spectrum than Schottky cells using either CuPc or TPyP, layer. Three-layered organic solar cells with an interlayer of co deposited dyes of p-type CuPc and n-type TPyP, between the respective dye layers were also prepared and characterized. They showed increased power conversion efficiency, due to the efficient carrier photogeneration in the enlarged photoactive region from the code posited layer. The spectral sensitization of a-Si:H solar cells using an organic layer was also obtained. The action spectrum was extended by 30 nm to longer wavelength range, using a 100 nm thick layer of TPyP. An exciton dissociation process explains the sensitization to the TPyP/a-Si:H interface, which gives rise of higher quantum efficiency at longer wavelengths. Hybrid structures like nanostructured ZnO/sensitized with CuPc dye/Au or CdTe nw's/ZnPc and CdTe nw's/TPyP, photovoltaic cells were fabricated and characterized too, few from them showing values of the external quantum efficiency more than 12% . However, those structures needs to be improved to increase their optical efficiency and charge collection. Finally, a few of the most new and performant experimental facilities in the field of preparation and characterization of photovoltaic cells of the **Research Development Centre for Materials and Electronic and Optoelectronic Devices of University of Bucharest** will be presented.*

*Keywords: organic semiconductors, photovoltaic cells, organic thin layers*

## 1. Introduction

In the latest 50 years, there has been considerable interest in the study of organic monomeric and polymeric material, as candidates for use in electronic and optoelectronic devices, especially organic photovoltaic cells [1-6].

There has been a great deal of interest in the photovoltaic properties of the organic semiconductors because of their potential use as inexpensive materials for solar cells. Their charge transport properties and the potential to absorb light practically in the whole range of the solar spectrum is due to the presence of  $\pi$ -electrons, able to move along the delocalized  $\pi$ -orbitals, resulting from  $sp^2$ -hybridization states of the carbon atoms. Even though the charge carrier mobilities of these materials are small ( $10^{-5}$  -  $1$   $\text{cm}^2/\text{Vs}$ ) as compared with inorganic semiconductors, their high absorption coefficients in visible region of the solar spectrum ( $\sim 10^5$   $\text{cm}^{-1}$ ), makes them good absorber materials for solar cells based on very thin films (50-100 nm) [7-9].

Unlike the case of inorganic semiconductors, in organic materials there is a relatively small diffusion length of excitons [10], due to their large binding energies [11,12], and consequently, stronger electric fields are required to dissociate them into free charge carriers, which will contribute to the photovoltaic response. Tacking into account these features of organic materials it is clear that only very thin organic layers must be used in efficient photovoltaic devices, then reducing their mass and consequently their cost, respectively. Even though most organic semiconductors are hole conductors with a relatively large optical band gap (1.5 - 3 eV), limiting the perfect match to whole solar spectrum, using the so called „tailoring ability” of chemical synthesis methods, the electrical and optical properties of the organic semiconductors can be changed continuously, making them promising, efficient and low cost materials for manufacturing of organic solar cells.

At the beginning, among the organic materials which have been studied for use in photovoltaic cells, small organic molecules of dyes (merocyanines, [1,2] phthalocyanines [7,13,14,15] and porphyrins [9,16,17] have mostly attracted the interest of scientists. In the latest 20 years, the development of new semiconducting polymers [18-20] determined their use into organic solar cells with continuously increased performances. [5]

As concerning the photovoltaic cell design, the first generation of organic photovoltaic cells was based on Schottky type devices, in which an organic layer is sandwiched between two electrodes having suitable work function, one of them forming a rectifying contact and the other one forming an ohmic contact with the dye layer [1,2,9,13,16,17]. There are some factors, which limit the performances of an organic Schottky cell. This type of cells generally exhibit a low power conversion efficiency, in the range ( $10^{-4}$ - $10^{-2}$ ), but have reached about 1% (exactly 0.7%) for merocyanine dyes, a promising result for the beginning of this field of research [1]. Higher power conversion efficiency, has been achieved with the two-layer organic photovoltaic cells [2,7,15,21-24]. Tang [21] reported in 1986 about 1% power conversion efficiency for double-layered organic photovoltaic cell, a result which was for many years the reference value for the organic photovoltaic cells, only surmounted at the beginning of this millennium, [23,24] when a

power conversion efficiency as high as 4.2% was reported [24] for the double-layered heterojunction CuPc/C60. In these devices, the interface between the two organic materials, rather than electrode/organic contacts, is crucial in determining the photovoltaic response. The absorption characteristics of the two layers, if complementary, enhance substantially the utilisation of wavelengths of solar spectrum by the two-layer cell as compared with single-layer cell.

At the beginning of last decade of the 20<sup>th</sup> century, an internal power conversion efficiency of 0.7% was reported by Hiramoto and co-workers [25], for a three-layered organic photovoltaic cell with a co-deposited interlayer between the p-type and n-type organic layers, which has been found to act as an efficient carrier photogeneration layer into a p-i-n like structure cell [26]. Afterwards, we have reported the strong “cosensitization” effect [7], presented by the two-layer organic photovoltaic cell fabricated from Copper Phthalocyanine (CuPc) as p-type organic semiconductor and 5,10,15,20-tetra-(4-pyridil)21H,23H-porphine (TPyP) as n-type organic semiconductor. Motivated by the encouraging results on heterojunction CuPc/TPyP devices and in an effort to obtain a thicker photoactive region at the interface between the two-organic layers, we have fabricated the ITO/CuPc/(CuPc+TPyP)/TPyP/Al three-layered organic cell, with a mixed layer of CuPc and TPyP between them.[27]

In the continuous search for new organic materials for photovoltaic applications, the field of conjugated polymers has attracted an increased interest and single layer cells based on these materials were already reported [28], but showing also less than 0.1% power conversion efficiencies.

It was been shown that in a conjugated polymers doped with C<sub>60</sub> molecules, a photoinduced electron transfer from optically excited conjugated polymers to C<sub>60</sub> molecules take place [29,30] and the polymer photoconductivity increases after C<sub>60</sub> addition [31]. These observations led to the development of two-layer cells based on polymer-fullerene [32,33] and to the concept of bulk heterojunction [34,35] containing as active sites the fullerene molecules or their derivatives [36].

The bulk heterojunction concept, similar to the above described co-deposited molecular structures [25-27] was then introduced, by mixing two polymers one having donor (D) properties (small ionization energy) and another with acceptor (A) properties (high electronic affinity), leading finally to a solid-state mixtures of both polymers, [37-39] or by the lamination of two polymer layers, leading to a diffusive interface between D and A compounds, with a calculated power conversion efficiencies on about 2%. [40]

At this stage, with these type of structures described above, we can talk on a real progress in the field of organic photovoltaic cells, because power conversion efficiencies more than 4% have been obtained for evaporated two-layered devices[24], bulk heterojunction polymer-fullerene devices,[41-44] co-evaporated molecular devices [45-47] and in organic-inorganic hybrid devices [48-51].

As referring to the last type of structures, it was demonstrated that hybrid structures made of inorganic nanoparticle systems and organic materials could represent an interesting and promising alternative for obtaining low-cost, high-efficiency solar cells. The most well known such a system is the dye-sensitized nanostructured solar cell developed by Grätzel. By the successful combination of nanostructured electrodes and efficient charge injection dyes, Grätzel and his co-workers have developed a solar cell with energy conversion efficiency exceeding 7% in 1991 and 10% in 1993.[52-56] This

solar cell is called *the dye sensitized nanostructured solar cell* or *Grätzel cell* after its inventor. In the recent years, by the introduction of organic hole conductors [56,57] as replacement for the liquid electrolytes in electrochemical solar cells and by the exchange of the electron conducting acceptor materials in integral-organic heterojunction devices with inorganic nanostructured films, [58-62] the way was opened to obtain high efficiency hybrid solid-state dye-sensitized solar cells. To reach this desiderate it is necessary a very high knowledge and understanding of the electrical and optical properties of the new organic and inorganic materials, potential candidates for photovoltaic applications together with the photovoltaic mechanisms in different design of the solar cells structure. In this chapter, we review the status of the organic photovoltaic cells produced in our laboratory, discussing permanently the factors which give rise to the improvements of their performance [67,68].

## **2. Sample Preparation and Measurements of Photovoltaic Cells.**

Most of the investigated cells were prepared using the following procedure. Indium tin oxide (ITO) coated glass provided the transparent conducting substrate (with transparency of 60% - 80%, for the average solar spectrum region), on top of which a layer of CuPc, TPyP, Chl-a with different thickness, was deposited by conventional vacuum evaporation. In the case of single-layer cells, a semitransparent top electrode was deposited on the organic layer, chosen to form an ohmic or blocking contact at the interface organic/metal. In the case of two-layer cells, the organic layer having p-type conductivity, was firstly deposited on ITO, and then over it the organic layer with n-type conductivity. Finally, a top electrode completed the structures. The deposition of the mixed interlayer, in the case of three-layer cells, was carried out by the co evaporation of CuPc and TPyP from two separated sources, on the first deposited CuPc layer. A third layer of TPyP having the same thickness, was deposited on top of the co deposited layer, also by vacuum evaporation. Finally, an Al layer having an area of  $0.25 \text{ cm}^2$ , was deposited by thermal vacuum evaporation, defining the active area of the cell. The cell configurations, were generally shown as insets in figures showing their dark current-voltages characteristics. Both CuPc and TPyP are thermally very stable, thus allowing their deposition by vacuum evaporation. During sublimation the source temperature was maintained at about  $380^\circ\text{C}$  for CuPc and at  $280^\circ\text{C}$  for TPyP. The ITO transparent electrode has been found to form an ohmic contact with p-type CuPc and Chl-a and the Al electrode a nearly ohmic contact with the n-type porphyrin [13,14]. The current-voltage (I-U) characteristics in the dark were measured by biasing the devices with a voltage stabilized power source. The current and voltage were measured with a Philips microammeter and a Keithley 614 electrometer, respectively. A 650 W halogen lamp provided the illumination of the cells. A monochromator (spectral range of 300 to 800 nm) was used to obtain the spectral responses. The optical absorption spectra of the organic layers were obtained on a Perkin Elmer UV-VIS spectrophotometer (Lambda 2S).

### 3. Experimental Results

#### 3.1. The mono-layer cells based on CuPc and TPyP

##### 3.1.1 ITO/CuPc/Al

The copper phthalocyanine (CuPc) is a p-type organic semiconductor having the hole equilibrium concentration  $p_0 = 2.3 \times 10^{13} \text{ cm}^{-3}$ , the mobility  $\mu_p = 1.1 \times 10^2 \text{ cm}^2/\text{Vs}$ , the dark electrical conductivity  $\sigma_p = 4 \times 10^{-8} \Omega^{-1} \text{ cm}^{-1}$  and the equilibrium Fermi level located at 0.455 eV above the valence band (VB), [8].

The prepared ITO/CuPc/Al cells [67-68] exhibit asymmetrical I-U characteristics, as a result of a contact barrier at Al/CuPc interface and an ohmic contact at ITO/CuPc interface (Fig. 1).

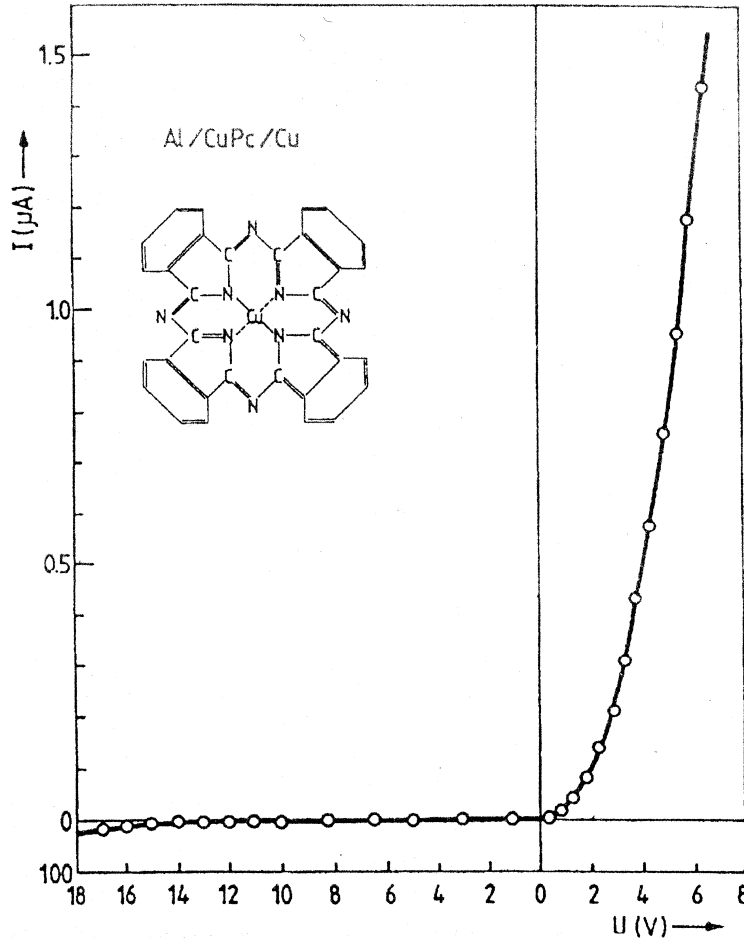


Fig. 1 Dark current-voltage characteristics of a ITO/CuPc/Al cell, at room temperature. The chemical structural formula of CuPc is shown in inset. Reprinted with permission from Ref. [67] S. Antohe, *Journal of Optoelectronics and Advanced Materials*, **2**, 498 (2000), Copyright INOE&INFM (2000)

The photovoltaic response is due to the charge carrier photogeneration in the organic layer and their separation in the electric field built at Al/CuPc interface.

The action spectra at illumination through the ITO electrode together with the absorption spectrum of the CuPc layer are shown in Fig. 2.

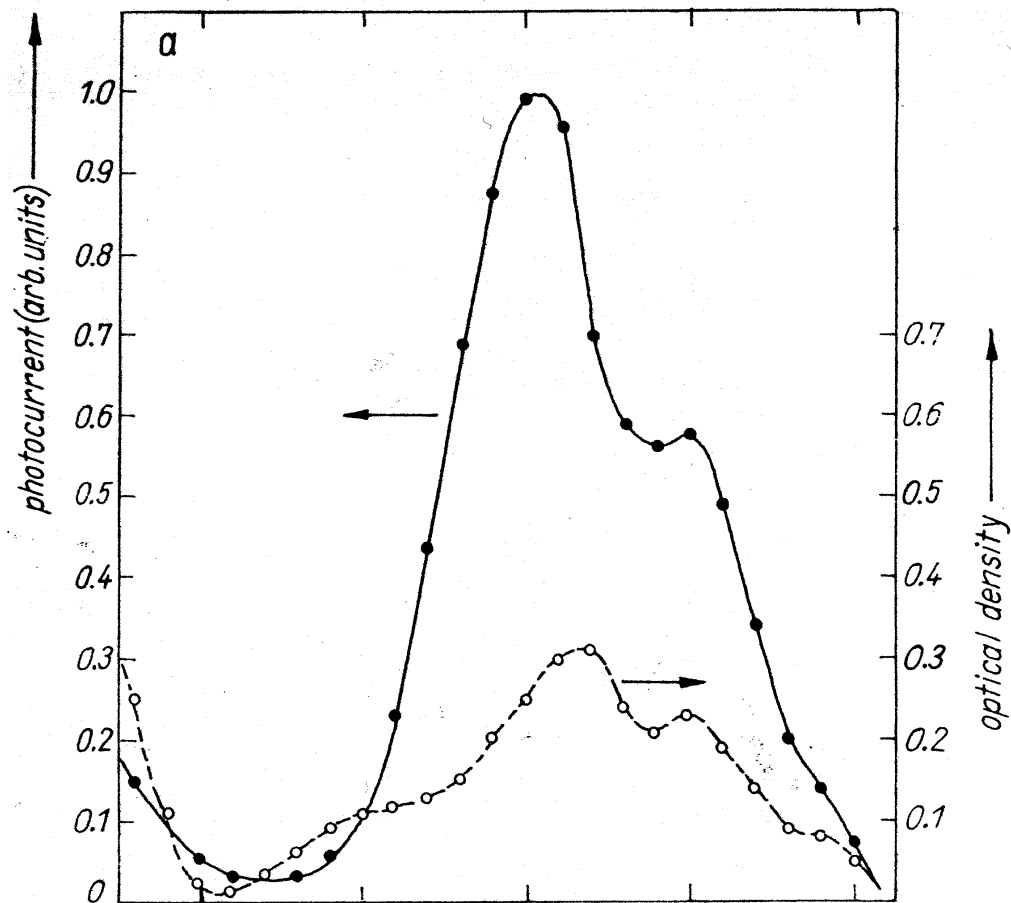


Fig. 2 Action spectrum of short - circuit photocurrent and absorption spectrum of the organic layers for the Schottky cells ITO/CuPc/Al. Reprinted with permission from Ref. [67] S. Antohe, Journal of Optoelectronics and Advanced Materials, **2**, 498 (2000), Copyright INOE&INFM (2000)

The typical cell parameters at illumination through ITO electrode with monochromatic light ( $\lambda = 620 \text{ nm}$  and  $\sim 10^5 \text{ photons/cm}^2 \text{ s}$ ) are: the open-circuit photovoltage  $U_{OC} = 0.675 \text{ V}$ , the short-circuit photocurrent  $I_{SC} = 8 \text{ nA}$ , and the fill factor  $ff = 0.35$ .

### 3.1.2 ITO/TPyP/Al

From the detailed analysis of dark Current-Voltage characteristics of ITO/TPyP/Al cells, described in section 1, resulted that the TPyP, differs from the majority of porphyrins and metal porphyrins in having n-type conductivity, due to the increase of electron affinity by the introduction of pyridil groups in place of phenyl groups. The asymmetry of I-U characteristics and as a consequence, the rectifying properties of the cells Fig. 3, [9] are due to a Schottky barrier at the ITO/TPyP interface while Al/TPyP is a Ohmic contact. I-U characteristics together with the absorption spectra of TPyP layer, are shown in Figure 3.

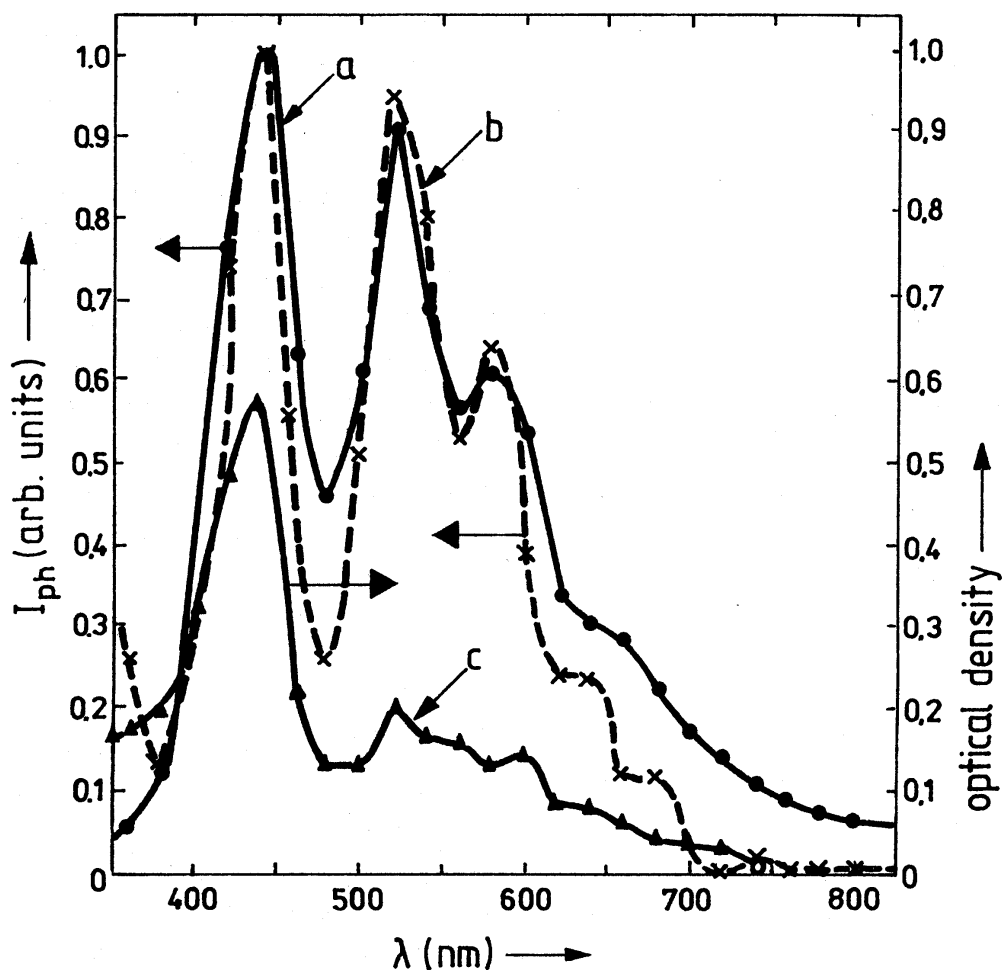


Fig. 3 Action spectra of the ITO/TPyP/Al photovoltaic cell and the absorption spectrum of the TPyP layer. Reprinted with permission from Ref. [67] S. Antohe, Journal of Optoelectronics and Advanced Materials, 2, 498 (2000), Copyright INOE&INFM (2000).

The action spectra, shown in Fig.3, and the photovoltaic response, can be explained by considering that the photogenerated carriers are separated in the built-in field, extended over the whole thickness of the organic layer. The typical cell parameters at illumination through ITO electrode with monochromatic light of  $32 \mu\text{W}/\text{cm}^2$  at  $\lambda = 440 \text{ nm}$  were: the open-circuit photovoltage  $U_{oc} = 0.175 \text{ V}$ , the short-circuit photocurrent  $J_{sc} = 42 \text{ nA}/\text{cm}^2$ , the fill factor  $ff = 0.13$  and the power conversion efficiency  $\eta_e = 0.27 \times 10^{-2} \%$ .

## 3.2. Two-Layer Organic Photovoltaic Cells

### 3.2.1. ITO/CuPc/TPyP/Al

The combination of the two organic layers CuPc and TPyP in the ITO/CuPc(80 nm)/TPyP(50 nm)/Al p-n heterojunction cell, Figure 4, led to an increase of power conversion efficiency by about two orders of magnitude, with respect to ITO/CuPc/Al and ITO/TPyP/Al mono-layer cells, as a result of a "cosensitization effect" [7].

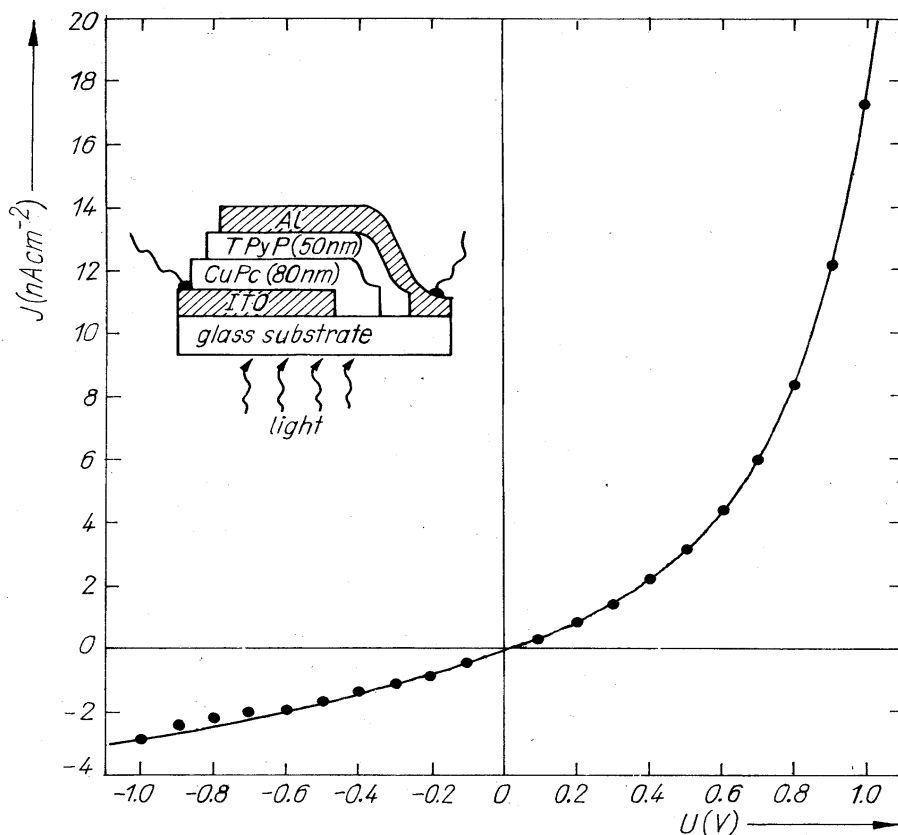


Fig. 4 Cell configuration (inset) and dark current-voltage characteristics of ITO/CuPc/TPyP/Al. Reprinted with permission from Ref. [14] S. Antohe and L. Tugulea, *phys. stat. sol. (a)* **128**, 253 (1991), Copyright WILEY-VCH Verlag GmbH & Co. KGaA, (1991)

Indeed the two organic layers with complementary absorption spectra are involved in the photogeneration processes. The action spectrum, shown in Figure 5, is larger than those of single layer cells (Figure 6). The resemblance of the two action spectra in Fig. 5, suggests that the region of maximum photosensitivity is at the CuPc/TPyP interface. A marked feature to be noted in Fig. 5a, is that curve 1 shows a distinct photocurrent maximum in the Soret band of TPyP film, while curve 2 has only a small peak around this band.

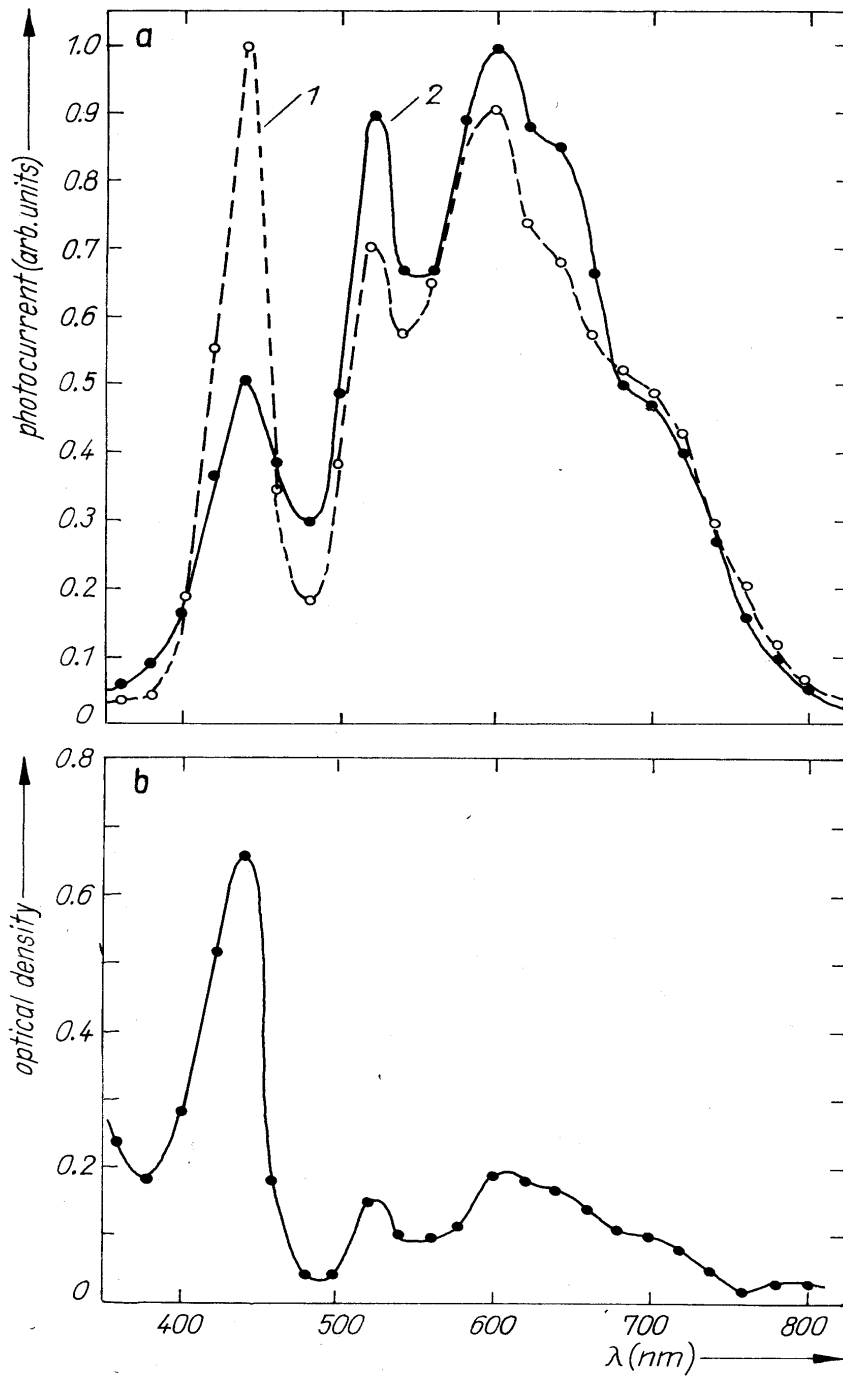


Fig. 5. a) Action spectra of short - circuit photo-current for the p-n junction cell of ITO/CuPc/ TPyP/Al. Curves (1) and (2) are obtained at illumination of the Al and ITO electrodes, respectively. (1)  $J_{ph\ 400\ nm} = 0.845\ nA/cm^2$ , (2)  $J_{ph\ 600\ nm} = 223\ nA/cm^2$ . b) Optical absorption spectrum of the CuPc/TPyP two layer film. Reprinted with permission from Ref. [14] S. Antohe and L. Tugulea, phys. stat. sol. (a) **128**, 253 (1991), Copyright WILEY-VCH Verlag GmbH & Co. KGaA, (1991)

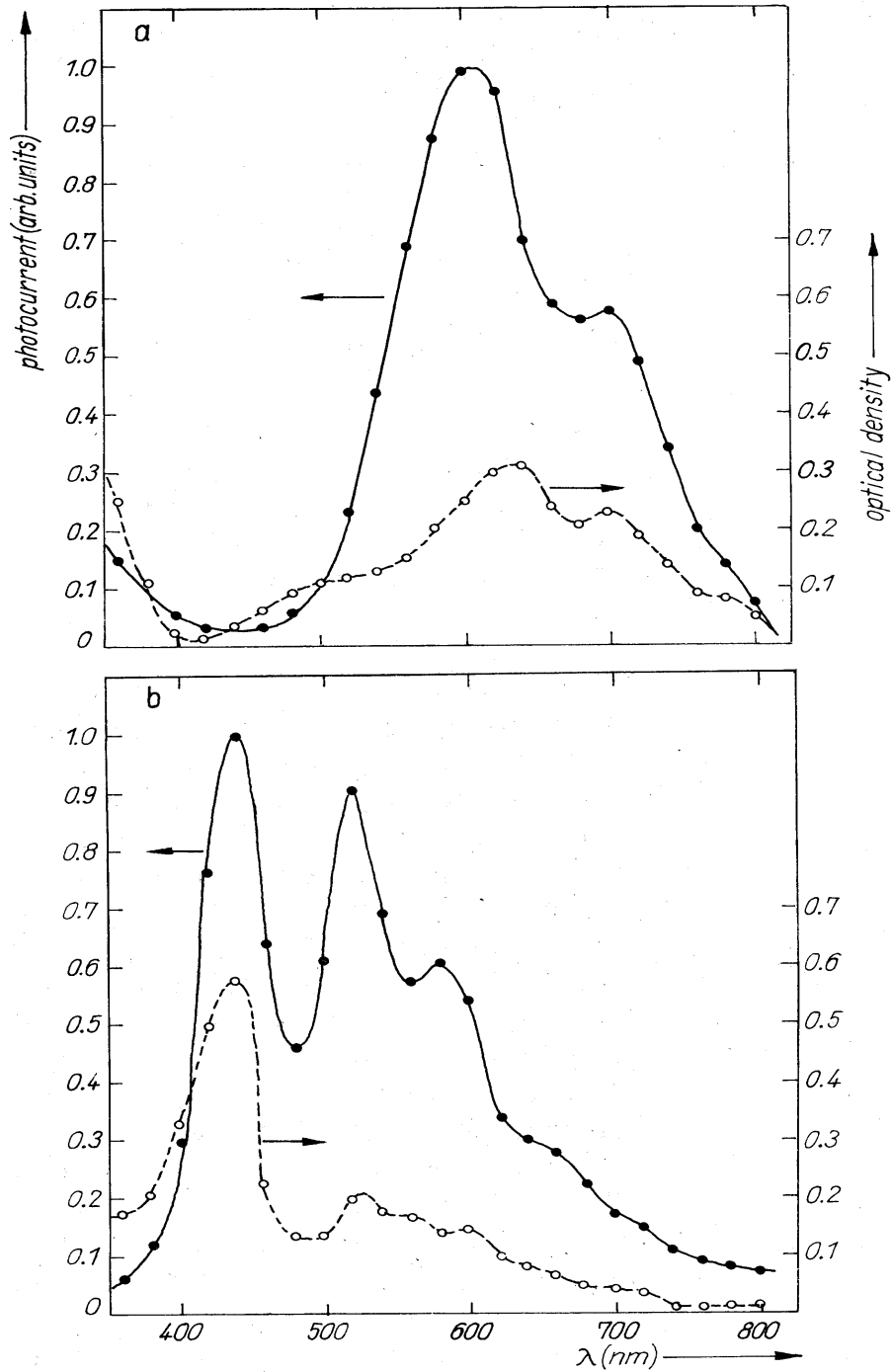


Fig.6. Action spectrum of short - circuit photocurrent for the Schottky cells of: (a) ITO/CuPc/Al; (b) ITO/TPyP/Al, at illumination through the ITO electrode, and the absorption spectrum of the: a) CuPc; b) TPyP layer . a)  $J_{ph\ 600\ nm} = 37.2\ nA/cm^2$ , b)  $J_{ph\ 440\ nm} = 28.8\ nA/cm^2$ . Reprinted with permission from Ref. [14] S. Antohe and L. Tugulea, phys. stat. sol. (a) **128**, 253 (1991), Copyright WILEY-VCH Verlag GmbH & Co. KGaA, (1991)

In addition, in curve 2, the observed photocurrents in the range of broad absorption bands of CuPc film at wavelength from 500 to 750 nm, are greater than those in curve 1. Assuming the photoactive region to be the interface CuPc/TPyP, the above features in the action spectra may be interpreted in the following way: photons strongly absorbed in the Soret band of TPyP, are responsible for the maximum of photocurrent in curve 1, but also photons weakly absorbed in TPyP are participating in the photogeneration in the region of internal field from CuPc layer. Since the CuPc layer is thicker than the TPyP films, the maximum of photocurrent is obtained at the maximum of absorption in CuPc while the small photocurrent peak at the Soret band of TPyP, may be caused by attenuation of light reaching the p-n junction through the CuPc phase. The J-U characteristic of the ITO/CuPc/TPyP /Al photovoltaic cell in the fourth quadrant of the J-U diagram is shown in Figure 7.

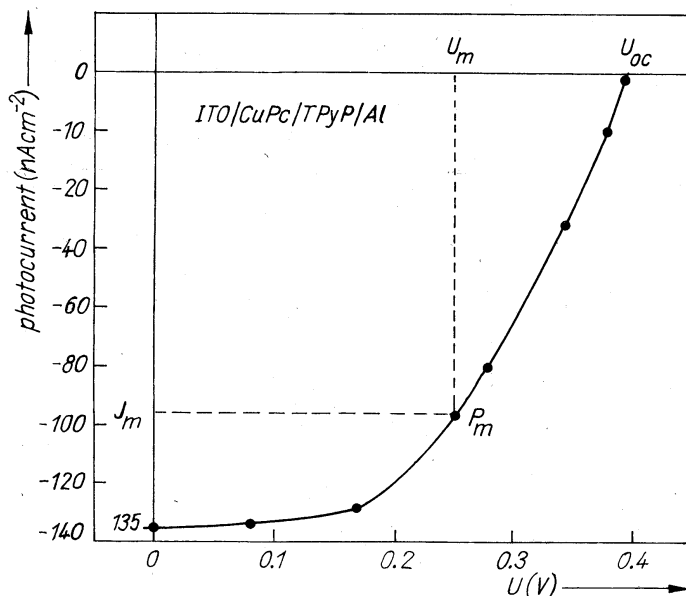


Fig. 7. Current - voltage characteristics for a ITO/CuPc/TPyP/Al photovoltaic cell in the fourth quadrant, under illumination with monochromatic light of  $20 \mu\text{W}/\text{cm}^2$  at 440 nm. Reprinted with permission from Ref. [14] S. Antohe and L. Tugulea, phys. stat. sol. (a) **128**, 253 (1991), Copyright Phys. Stat. sol.(a) (1991)

The cell was illuminated in monochromatic light of  $20 \mu\text{W}/\text{cm}^2$  at 440 nm and the charge resistors were varied in the range of 100 k $\Omega$  to 2 T $\Omega$ . The typical cell parameters have the following values:  $U_{oc} = 400 \text{ mV}$ ,  $J_{sc} = 135 \text{ nA}/\text{cm}^2$ ,  $ff = 0.44$  and  $\eta_e = 0.12\%$ . The best power conversion efficiency, obtained under such illumination condition and without correction for the reflection or electrode absorption losses, was about 100 times greater than that for organic monolayer cells.

The obtained value of the fill factor represents a substantial improvement as compared with the values of 0.12 and 0.13 obtained for single-layer cells ITO/CuPc/Al and

ITO/TPyP/Al, respectively.

As concerning the model of operation, it was assumed that the absorption of light by both CuPc and TPyP layers creates excitons, which can diffuse in the bulk of the films.

At the interface or junction between the CuPc and TPyP layers the dissociation of excitons can take place, generating charge carriers. Therefore, holes are preferentially transported in the CuPc layer by the built-in field in p-n junction and are collected by the ITO electrode, while the electrons are transported in the TPyP layer towards the Al electrode. The observed polarity of the photovoltage, i.e. the CuPc layer is always positive with respect to the TPyP layer regardless of the electrode materials, is strongly indicative of conduction type in the two layers [7-9].

### 3.2.2. ITO/Chlorophyll a /TPyP/Al

Figure 8 shows the dark-current density through a typical ITO/Chla(200 nm)/TPyP(100 nm)/Al cell as function of applied bias at room temperature [63,64].

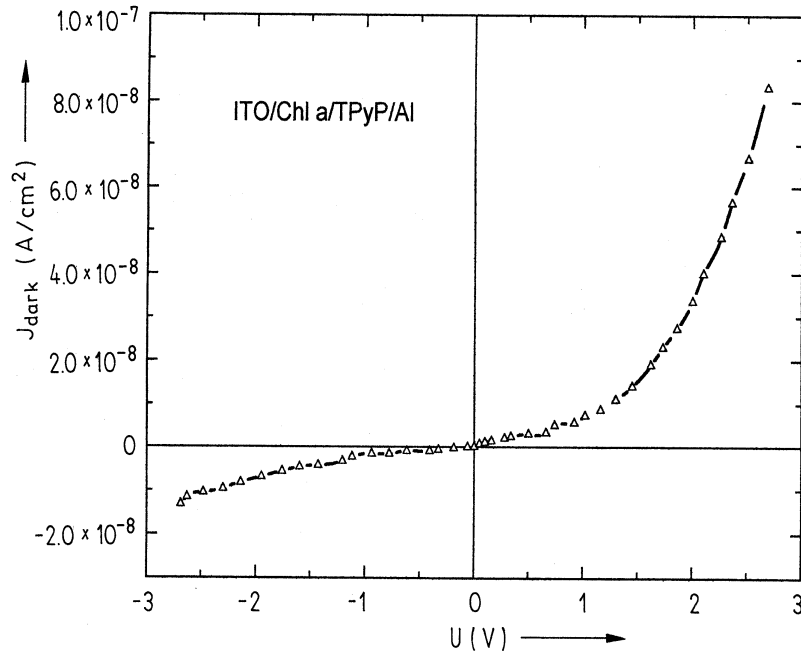


Fig. 8. Current - voltage characteristic of ITO/Chl a(200 nm)/TPyP (100nm) cell in the dark at room temperature. Reprinted with permission from Ref. [93] S. Antohe, L. Tugulea, V. Gheorghe, V. Ruxandra, I. Caplanusi and L. Ion, *phys. stat. sol. (a)* **153**, 581 (1996), Copyright WILEY-VCH Verlag GmbH & Co. KGaA, (1996)

Chla is considered to be a p-type semiconductor, with high work function of  $\sim 4.5$  eV and the ITO electrode, having a work function of about  $\sim 4.7$  eV forms an ohmic contact at the interface ITO/Chla. TPyP being a n-type semiconductor, with a low work function of  $\sim 4.1$  eV [7], forms an ohmic contact with Al. Since Chla and TPyP make ohmic contacts with ITO and Al electrodes, respectively, we infer that the rectification shown in the bipolar J-U characteristic in Fig.8, is due to the energy barrier at the Chla/TPyP interface.

Figure 9b shows the action spectrum of the p-n heterojunction cell ITO/Chla(200nm)/TPyP(100nm)/Al (1), together with the action spectra of the Schottky type cells : ITO/Chla(200nm)/Al (2) and ITO/TPyP(100nm)/Al (3), respectively. All the spectra are obtained by illumination on the ITO electrode. Fig. 9a shows the optical absorption spectrum of Chla/TPyP (a), Chla (b) and TPyP (c) films, respectively, used in the fabrication of sandwich cells. For all action spectra in Fig. 9b the photocurrents are divided by the number of photons incident on the ITO electrode for each wavelength and then normalized to unity.

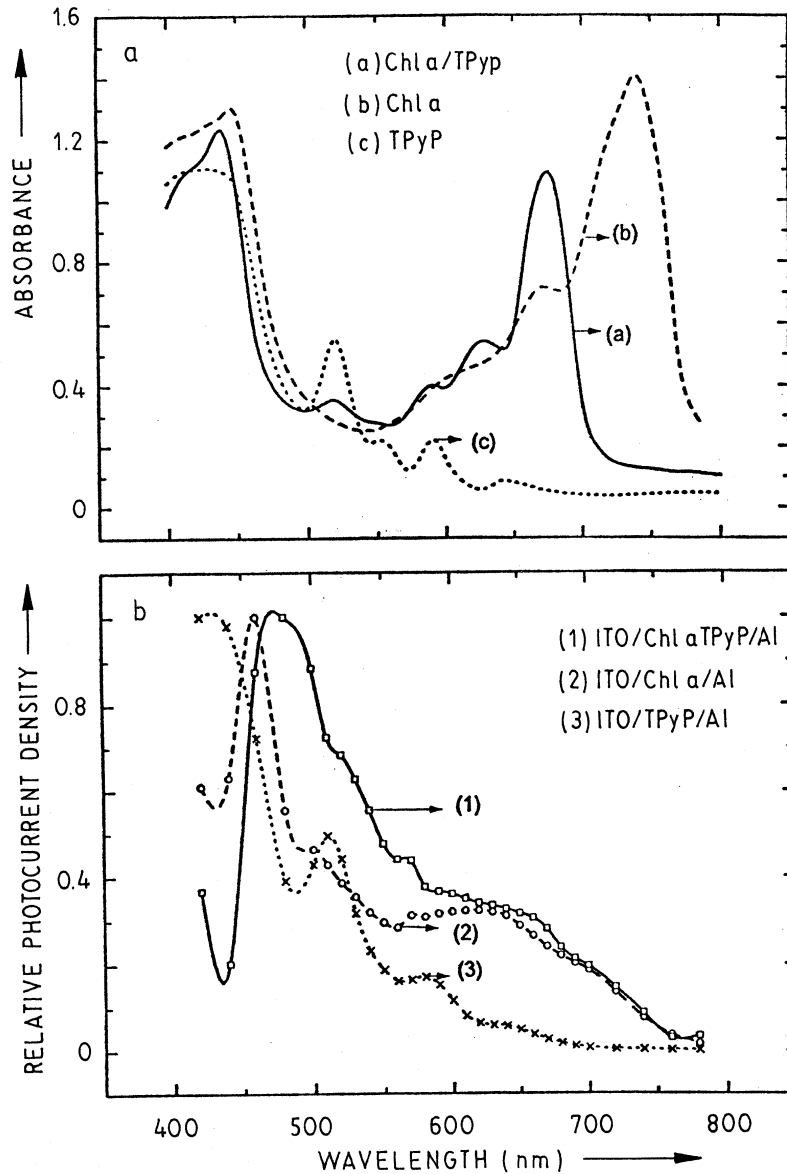


Fig. 9. a) Absorption spectrum of Chl a/TPyP films, Chl a layer, and TPyP layer. b) Action spectra of cells illuminated through ITO: ITO/Chl a/Al (1), ITO/Chl a/Al (2), and ITO/TPyP/Al (3). Reprinted with permission from Ref. [93] S. Antohe, L. Tugulea, V. Gheorghe, V. Ruxandra, I. Caplanusi and L. Ion, *phys. stat. sol. (a)* **153**, 581 (1996), Copyright WILEY-VCH Verlag GmbH & Co. KGaA, (1996)

The action spectrum of the two-layer cell, when illuminated through ITO electrodes matches better the absorption spectrum of TPyP film than of Chla film. This behavior suggests that the singlet excitons are the precursors of the charge carriers and that the space-charge region is at the Chla/TPyP interface. In other words, only those excitons created in the barrier region or having diffused into it contribute to the photocurrent. The photocurrent generation in the p-n heterojunction cell, as compared with that in the Schottky cells (Fig. 9b, curves (2) and (3)), is strongly enhanced at the wavelengths corresponding to the absorption peaks of the organic and biologic layer. The photocurrent measured at 460 nm is about three times greater in the case of ITO/Chla/TPyP/Al cell than that of ITO/Chla/Al cell, while the photocurrent of p-n heterojunction cell measured at 670 nm is about seven times greater than that of ITO/TPyP/Al cell. The appearance of a large photocurrent at wavelengths corresponding to the Soret region of Chla absorption spectrum can be explained by the photogeneration of charges in TPyP layer in addition to the charge generation in Chla layer. The larger photocurrent of p-n heterojunction cell at 670 nm is due to the charges photogenerated mostly in Chla layer. All the compared action spectra were obtained at illumination through the ITO electrode. The ratio of area covered by the action spectra of ITO/Chla/TPyP/Al, ITO/Chla/Al and ITO/TPyP/Al cells is 144:123:87 (Fig. 9b), pleading for a "cosensitization effect" in the case of ITO/Chla/TPyP/Al two-layer cell. The fourth quadrant of J-U characteristic of ITO/Chla/TPyP/Al photovoltaic cell at illumination with monochromatic light of  $20 \mu\text{W}/\text{cm}^2$  at 470 nm, leads to the photovoltaic cell parameter values:  $U_{OC} = 490 \text{ mV}$ ,  $J_{SC} = 13 \text{ nAcm}^{-2}$  and  $ff = 0.34$ . The fill factor of 0.34 represents a substantial improvement as compared with the values of 0.09 and 0.13 obtained for ITO/Chla/Al and ITO/TPyP/Al Schottky cells, respectively. The power conversion efficiency, obtained under the mentioned conditions of illumination and without correcting for reflection or electrode absorption losses, was  $\sim 1.1 \times 10^{-2}\%$ , about 2-3 times higher than the value obtained for ITO/Chla/A cell. The conversion efficiency is strongly limited by the high internal resistance,  $\sim 200 \text{ M}\Omega$ , due to the thickness of Chla and TPyP films.

### 3.3 Three - Layered Photovoltaic Cell with an Enlarged Photoactive Region of Codeposited Dyes

#### 3.3.1. ITO/CuPC/(CuPc+TPyP)/TPyP/Al

##### a) Dark current-voltage characteristics

Fig.10 shows the dark current through a typical ITO/CuPc/(CuPc+TPyP)/ TPyP /Al cell as a function of the applied bias, at room temperature Antohe et al. [27]

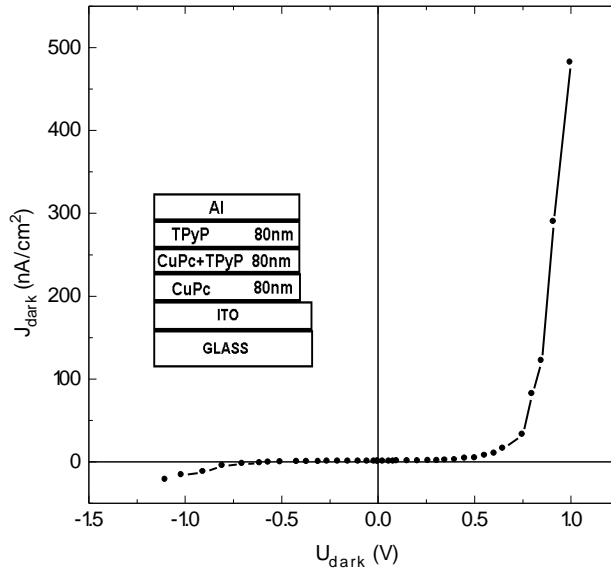


Fig. 10. Cell configuration (inset) and the dark current-voltage characteristics of the ITO/CuPc/(CuPc+TPyP)/TPyP/Al cell at room temperature. Reprinted with permission from Ref. [57] S. Antohe, V. Ruxandra, L. Tugulea, V. Gheorghe and D. Ionascu, *J. Phys. III France* **6**, 1133 (1996), Copyright EDP Sciences (1996)

The forward bias corresponds to a positive voltage on ITO with respect to Al electrode. The cell exhibits a strong rectifying effect in the dark, characterised by the rectification ratio (forward bias current/reverse bias current) of nearly 500 at the voltage of 1 V. For a rigorous analysis of (I-U) curves with respect to conduction mechanisms and cell parameters, firstly we found out the implication of Shockley mechanism by seeking out the linear region in the  $\ln(I)$ -U plot of the forward current-voltage characteristics of the cell. The forward characteristic of the cell up to 1V can be fitted well by the modified Shockley equation:

$$I = I_0 \left\{ \exp \left[ \frac{q(U - IR_s)}{nkT} \right] - 1 \right\} + \frac{U - IR_s}{R_{sh}} \quad (1)$$

where:  $I_0$ ,  $n$ ,  $R_s$  and  $R_{sh}$  are the reverse saturation current, diode quality factor, series and shunt resistance of the cell, respectively, and  $q$  is the electronic charge.

From Eq.(1), the junction resistance,  $R_0$ , is:

$$R_0 = dU/dI = R_s + 1/\{\beta I_0 \exp[\beta(U - IR_s)] + 1/R_{sh}\} \quad (2)$$

where  $\beta = q/nkT$ .

For higher forward bias, where  $R_s$  affects the curves, equation (1) can be approximated as  $I = I_0 \exp[\beta(U - IR_s)]$ , and since  $1/R_{sh} < \beta I$ , equation (2) can be written as:

$$R_0 \cong R_s + 1/\beta I \quad (3)$$

Thus by plotting  $R_0$  vs  $1/\beta I$  for high forward biases, one can obtain  $R_s$  and the value of  $n$ . For low voltages, where  $R_{sh}$  acts, the approximation  $\beta I_0 \exp[\beta(U - IR_s)] \ll 1/R_{sh}$  is valid, and equation (2) becomes:

$$R_0 \cong R_s + R_{sh} \quad (4)$$

Usually  $R_s \ll R_{sh}$ ,  $R_0$  thus approaches  $R_{sh}$  at low biases. The graph of  $R_0$ , the junction resistance, versus  $1/I$  is shown in Fig.11, for one of our three-layered cell.

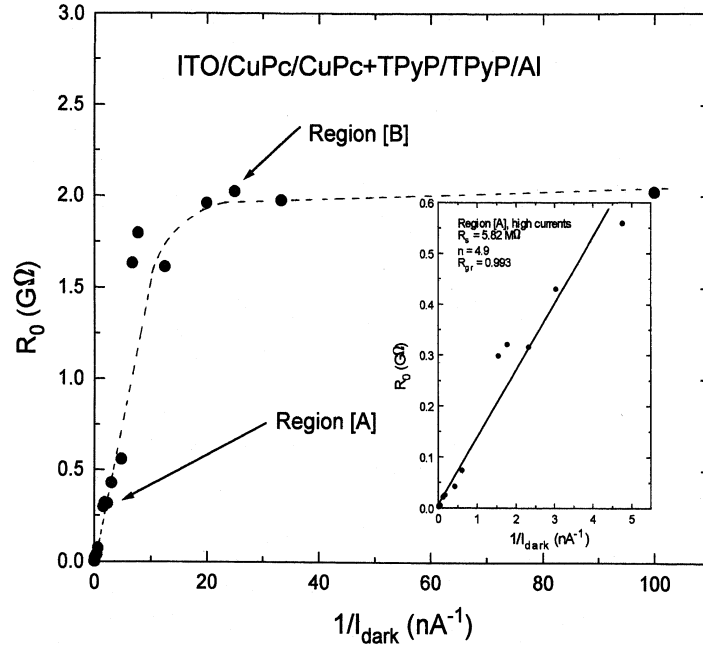


Fig. 11. The variation of junction resistance  $R_0$  as a function of reciprocal forward current  $1/I$ . The insert zooms on region A of high currents. Reprinted with permission from Ref. [57] S. Antohe, V. Ruxandra, L. Tugulea, V. Gheorghe and D. Ionascu, *J. Phys. III France* **6**, 1133 (1996), Copyright EDP Sciences (1996)

One can divide the plot in two regions: [A] and [B], for high and low forward currents, respectively. For region [A] (expanded in the inset), one notices that  $R_0$  as a function of  $1/I$  shows linearity up to the applied voltage of  $\sim 0.7$  V (the voltage from J-U plot in Figure 11, corresponding to the value  $0.6 \text{ G}\Omega$  of  $R_0$ ) and curves thereafter, for high forward biases. From the extrapolated linear region [A], the determined value of  $R_s$  is  $5.82 \text{ M}\Omega$ , the value of  $R_{sh}$ , obtained from region [B] being  $\sim 2 \text{ G}\Omega$ . These values of  $R_s$ ,  $n$  and  $R_{sh}$ , depending upon experimental conditions are comparable to those obtained by other authors for organic photovoltaic cells.[69,70]

To improve the linearity of  $\ln(I)$ - $U$  plot, for determination of  $n$  and  $I_0$ , we firstly removed the effect of  $R_s$ . This was achieved by making the following change in variable:

$$Y = U - IR_s \quad (5)$$

With this change, equation (1) becomes:

$$I = I_0[\exp(\beta Y) - 1] + Y/R_{sh} \quad (6)$$

where  $Y$  is the voltage only across the junction. For high forward biases, equation (6) can be written as:

$$I \cong I_0 \exp(\beta Y) \quad (7)$$

Thus, from the plot of  $\ln I$  vs.  $Y$ ,  $n$  and  $I_0$  can be determined. Further, to increase the precision it is advisable to remove the effect of  $R_{sh}$  from the  $\ln(I)$ - $U$  plot, as well. This is achieved by plotting  $\ln(I - Y/R_{sh})$  vs.  $Y$ , because  $(I - Y/R_{sh})$  can be considered to describe the current flowing in the diode junction only. Such a plot is shown in Fig.12a. One can see that the removal of  $R_{sh}$  and  $R_s$  has led to the increase in the linearity of the curve at lower biases from 0.3V to 0.1V and at higher biases from 0.7 to 0.8 V, respectively. Then the whole linear region of  $\ln(I)$ - $U$  plot is extended in the range 0.1-0.8V. The values of  $n$  and  $I_0$  obtained from the slope and the intercept are 2.79 and  $6.2 \times 10^{-13}$  A, respectively and are more reliable than those obtained after the removal of  $R_s$  only. For biases  $> 0.8$ V, the current shows a power dependence of voltage, i.e. follows the relation  $I \sim U^m$  where  $m = 7$ , as seen from  $\log(I)$ - $\log(U)$  plot in Fig.12b. This super quadratic power dependence suggests that the dark current is a space-charge-limited-current (SCLC) in the presence of exponentially distributed traps.

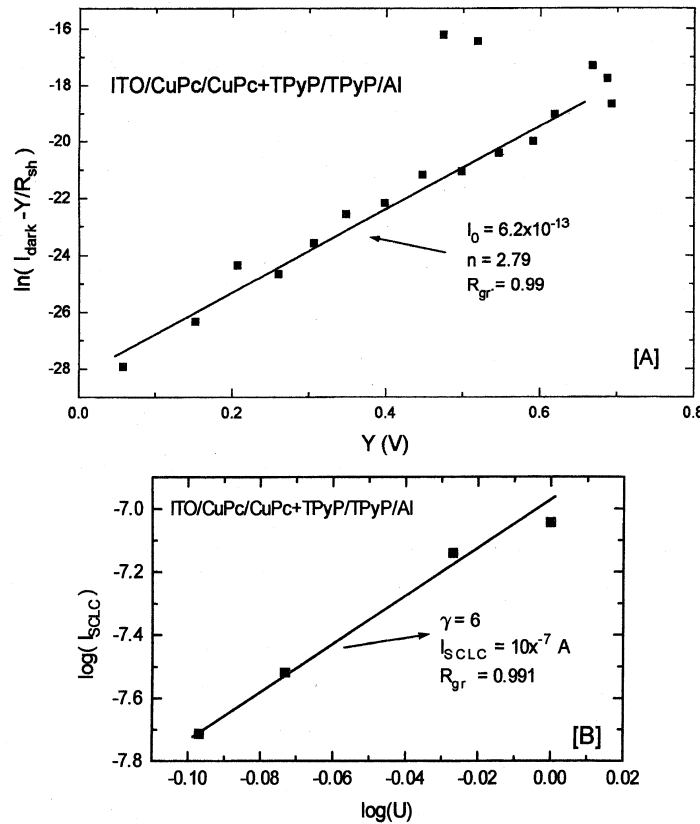


Fig. 12. [A] Semi logarithmic plots of the forward-biased dark current:  $I - Y/R_{sh}$  vs  $Y$ . [B] Logarithmic plot of SCLC current vs voltage for high forward biases. Reprinted with permission from Ref. [57] S. Antohe, V. Ruxandra, L. Tugulea, V. Gheorghe and D. Ionascu, *J. Phys. III France* **6**, 1133 (1996), Copyright EDP Sciences (1996)

According to Mark and Helfrich [95], the SCLC for a solid with a trap distribution decreasing exponentially with the trap depth is given by:

$$J_{\text{SCLC}} = N_{\text{eff}} \mu q^{1-\gamma} [\varepsilon \gamma / N_t (\gamma + 1)]^\gamma [(2\gamma + 1) / (\gamma + 1)]^{\gamma + 1} (U^{\gamma + 1} / d^{2\gamma + 1}) \quad (8)$$

where  $N_{\text{eff}}$  is the effective density of states in conduction or valence band, and  $\gamma = T_c / T$ , where  $T_c$  is a “characteristic temperature”, that describes the trap distribution.

#### b) The Photovoltaic Properties

The photovoltaic action spectra can provide considerable information as regarding to how the charge carriers are generated. The action spectra of short-circuit photocurrents of ITO/CuPc/(CuPc+TPyP)/TPyP/Al and ITO/CuPc/TPyP/Al cells are shown in Figs.13a and 13b, while the absorption spectra of the organic layers CuPc and TPyP are shown in Fig.6.

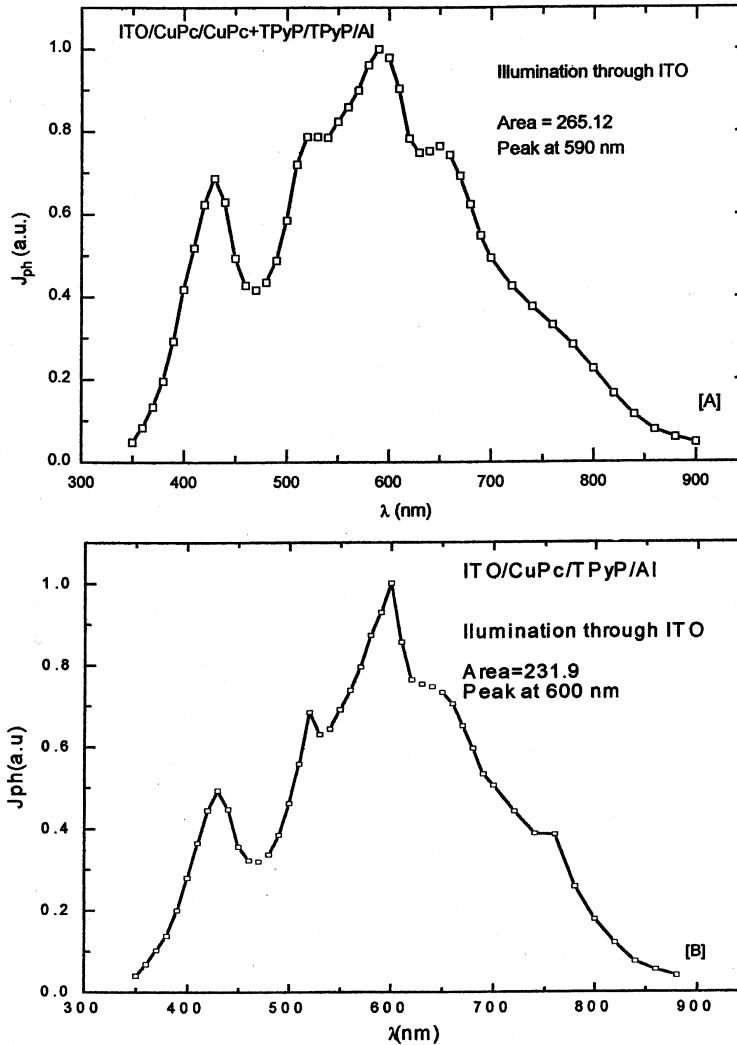


Fig. 13. The action spectra of the cells: [A] ITO/CuPc/(CuPc+TPyP)/TPyP/Al; [B] ITO/CuPc/TPyP/Al, illuminated through ITO electrode. Reprinted with permission from Ref. [57] S. Antohe, V. Ruxandra, L. Tugulea, V. Gheorghe and D. Ionascu, *J. Phys. III France* **6**, 1133 (1996), Copyright EDP Sciences (1996)

The action spectra are measured at illumination through the ITO electrode. Although the absorption spectra of TPyP and CuPc layers, are nearly complementary (the main

maxima of TPyP and CuPc layers are centered at 430 and 620 nm, respectively), both the TPyP and CuPc layers contribute to the photogeneration of carriers in the two cells. A marked feature to be noted in Fig.13 is that both curves show greater photocurrents in the range of the broad absorption band of CuPc film (at wavelength between 500 and 750 nm). In the Soret region of all action spectra presented in Fig.13, a distinct peak appears, as a result of the photons weakly absorbed in CuPc, but strongly absorbed in the Soret band of TPyP. It is important to note that, although both TPyP and CuPc layers show a moderate absorption at wavelength of 520nm (Fig.6), a peak of photocurrent exists at this wavelength, which is greater than that from Soret band of TPyP. The filtering effect of CuPc layer has to be considered. This behavior shows strongly that the photoactive region (i.e. in the internal field region) there is at the CuPc/TPyP interface. The photocurrent of the three-layered cell (Fig.13a), was about ten times larger than that of two-layered cell (Fig.13b) all over the spectral region. The thickness of the front CuPc layers is the same (80 nm) in both typed cells, i.e. the same masking effect due to CuPc layer. This result strongly suggests that the codeposited interlayer, which has a large amount of direct molecular contacts between TPyP and CuPc molecules and consequently a thicker depletion region, may provide an efficient carrier photogeneration layer. It is known [2] that an efficient photogeneration mechanism is that of exciton dissociation on the doping complex states present in the volume of an organic photoconductor. That is why, presently, we suspect that the charge photogeneration via exciplex of the two dyes, i.e.  $(TPyP^- \dots CuPc^+)^*$ , from codeposited layer is responsible for the efficient photogeneration of the charge carriers. The better agreement of the absorption spectrum of the codeposited layers and the action spectra of the cells illuminated through ITO electrode, suggests that the singlet excitons are the precursors of the charge carriers by the previous described process and that the photovoltaic region is located in the co deposited interlayer.

The dependence of the short-circuit photocurrent ( $J_{sc}$ ) on the incident light intensity ( $I_{inc}$ ), when illuminated through ITO, was examined too. At the wavelengths 520 and 590 nm, the dependence of ( $J_{sc}$ ) vs ( $I_{inc}$ ) of the cell follows the relation  $J_{sc} \sim I_{inc}^m$ , where the exponent  $m < 1$ . This is a common behavior for the organic photovoltaic cells and could be explained by taking into account the model based on the combined effect of traps and recombination centers. [7,13, 14,16]

Figure 14 shows the ( $J_{ph}$  -U) characteristics in the fourth quadrant of (J-U) diagram of a typical ITO/CuPc/(CuPc+TPyP)/TPyP/Al cell, obtained at 520 and 590 nm, the wavelengths where a high sensitivity of the cell exists.

These curves were obtained by varying the load resistance in the range 100 k $\Omega$  to 2 T $\Omega$  at constant input light intensities, which are given in the legend of each plot. Several parameters of interest, such as open-circuit photovoltage ( $U_{oc}$ ), short-circuit photocurrent ( $J_{sc}$ ), fill factor (ff) and power conversion efficiency ( $\eta$ ) can be evaluated from these curves.

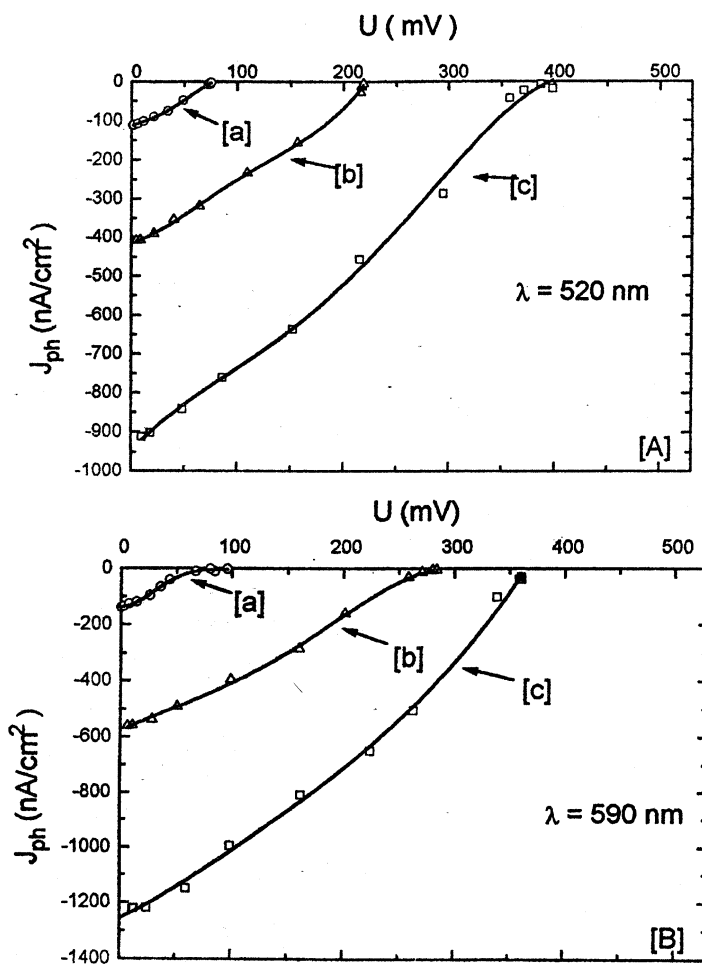


Fig. 14 Photocurrent- photovoltage characteristics of the ITO/CuPc/(CuPc+TPyP)/TPyP/Al cell illuminated through ITO electrode with: [A] 520 nm wavelength of varying intensity as ( $3 \mu\text{W}/\text{cm}^2$  [a],  $12 \mu\text{W}/\text{cm}^2$  [b] and  $30 \mu\text{W}/\text{cm}^2$  [c]); [B] 590 nm wavelength of varying intensity as ( $6 \mu\text{W}/\text{cm}^2$  [a],  $30 \mu\text{W}/\text{cm}^2$  [b] and  $72 \mu\text{W}/\text{cm}^2$  [c]). Reprinted with permission from Ref. [57] S. Antohe, V. Ruxandra, L. Tugulea, V. Gheorghe and D. Ionascu, *J. Phys. III France* **6**, 1133 (1996), Copyright EDP Sciences (1996)

The fill factor defined as ratio of the maximum output power density to the ( $U_{oc} * J_{sc}$ ) product, gives a measure of how close the cell is to an ideal photovoltaic cell ( $ff = 1$ ). The fill factors of this particular cell have different values ranging from 0.11 to 0.32. The low fill factors obtained for this cell are comparable to other organic photovoltaic cells, [7,13,15,22] but generally larger than of single and two-layered organic cells. These low values are due to two separate effects, namely, the high series resistances and the field-dependent nature of the photogeneration of charge carriers. [2,17] The highest value of fill factor was obtained at 520 nm for  $3 \mu\text{W}/\text{cm}^2$ , and smaller values were obtained for higher light intensities at all wavelengths.

The power conversion efficiency has been evaluated from the following relation

$$\eta(\%) = \frac{ff \times J_{sc} \times U_{oc}}{I'_{inc}} \times 100 \quad (9)$$

where  $I'_{inc}$  is the light power density incident on the cell corrected for the transparency of ITO electrode. The efficiencies were evaluated at 520 and 590 nm, for various values of the input power. The best performances of the cell are obtained for more penetrating 520 nm wavelength where the values 0.09, 0.22 and 0.35% for 3, 12 and 30  $\mu\text{W}/\text{cm}^2$  input powers have been obtained. These values of  $\eta$  are about 2-3 times larger than those of a two-layer cell. A better performance of the cell at shorter wavelength is most probable due to the bulk ionization of more energetic 520 nm excitons into charge carriers, mainly in TPyP layer. One can observe that for this wavelength the efficiency increases when the light intensity increases. At longer wavelength, such as 590 nm, the efficiency increases when the intensity increases up to 30  $\mu\text{W}/\text{cm}^2$  and decreases when the light intensity increases further. This decrease is mostly due to the above evaluated dependence of  $J_{sc}$  on  $I_{inc}$  and can be understood in terms of a physical model involving traps and recombination centers. [66] As the light intensity is increased, the electron and hole densities increase and therefore the quasi-Fermi levels are moving toward the conduction and valence bands, respectively. As the light intensity is further increased, more and more of the trapping states are converted into recombination centers, thus reducing the lifetime of charge carriers and resulting into non-linear variation of photocurrent with light intensity. As regarding the open-circuit photovoltage, both double- and three-layered cells showed almost the same magnitude for  $U_{oc}$ , about 0.4 V as an average value. This result tells us that the built-in potential for both typed cells originates from the difference of Fermi levels between CuPc and TPyP layers. We suppose that most of built-in potential is distributed across the interlayer. Since positive charges of ionic donors in n-type TPyP and negative charges of ionic acceptors, in p-type CuPc are compensated with each other, the co deposited layer behaves like an intrinsic semiconductor and then the three-layered cell resembles with a p-i-n a-Si:H based solar cell.

As a conclusion, this new type of three-layered organic photovoltaic cells having a co deposited layer of (CuPc +TPyP), between the CuPc and TPyP films, clearly suggest an improvement, although modest, over two-layered cells. The co deposited interlayer, has been found to act as an efficient carrier photogeneration layer because: on the one hand, the built-in potential drops across it and, on the other hand, here there is the region of maximum photogeneration rate, as a result of exciton dissociation via the exciplex of  $(\text{CuPc}^- \dots \text{TPyP}^+)^*$  dyes. The fill factors of 0.11-0.32 represent an improvement over single and double-layered cells. Moreover, the power conversion efficiencies of three-layered cells, ranging from 0.07 to 0.35%, are 2-3 times greater as compared to those for double-layered cells. The thickness of about 0.4  $\mu\text{m}$  of our three-layered cells is mainly responsible for the high internal resistance, which limits again the performances of the cells. By obtaining of an optimized structure as regarding the thickness of the layers and the architecture of the cells, substantial improvement of the organic photovoltaic cells would be possible.

### 3.4 Electrical and photovoltaic properties of photosensitized ITO/a-Si:H p-i-n/TPyP/Au cells

Hydrogenated amorphous silicon, a-Si:H, is of increasing technological interest for applications such as photovoltaic devices [71,72], due to two basic considerations: first, this material can be readily fabricated into large area, low-costs structures, and second the electrical and mechanical properties of a-Si:H are well suited for applications which require high radiation sensitivities and long device lifetimes. However, as regarding the applications in the photovoltaic systems, a fundamental limitation of a-Si:H is that the band gap is large (approximately 1.70 eV). As a result, a-Si:H shows little photoconductivity in the near infrared region of the spectrum, which is particularly important in the case of the solar radiation. The a-Si:H shows a photoconductive response very similar to the absorption spectrum, having also a photoconducting absorption edge [73]. Since the long wavelength absorption edge is believed to be determined by structural disorder there have been attempts to extend the absorption by controlling the degree of disorder, and an extension of the wavelength edge of the action spectrum to about 740-760 nm was already obtained in such a manner. On the other hand, there were attempts to obtain a spectral sensitization of a-Si:H by combining it with other elements such as Ge [74] or Sn [75] to form alloys with smaller band gaps. But also these materials have some fundamental limitations such as very low photogeneration efficiencies as compared to a-Si:H and increased dark conductivity. An efficient method of spectral sensitization of the action spectrum was indicated by Borsenberger [22]. He proposed to use the organic dyes or pigments as spectral sensitizers. By this technique the long-wavelength edge of the photoconductive action spectrum was extended by approximately 100 nm into near infrared using two organic layers: bromoindium phthalocyanine (as spectral sensitizer) and 1,1-bis (4-di-p-tolylaminophenyl)-cyclohexane (as chemical sensitizer).

Despite the interest in extending the action-spectrum of a-Si:H based solar cells to longer wavelengths, there have been no reported attempts to spectrally sensitize these cells by the Borsenberger's technique. That is why we investigated the spectral sensitization of the a-Si:H p-i-n solar cells, using as spectral sensitizer an organic layer of 5,10,15,20-tetra (4-pyridyl) 21H,23H porphine (TPyP), [48], showing that TPyP acts as spectral sensitizer for the a-Si:H p-i-n solar cells, giving some gains for the typical cell parameters, but its presence modifies the electrical behavior of the cell.

The dark current-voltage ( $I_d$ -U) characteristics of the ITO/a-Si:H p-i-n/TPyP/Au is shown in Fig.15, containing as inset the cross section of the cell. [48]

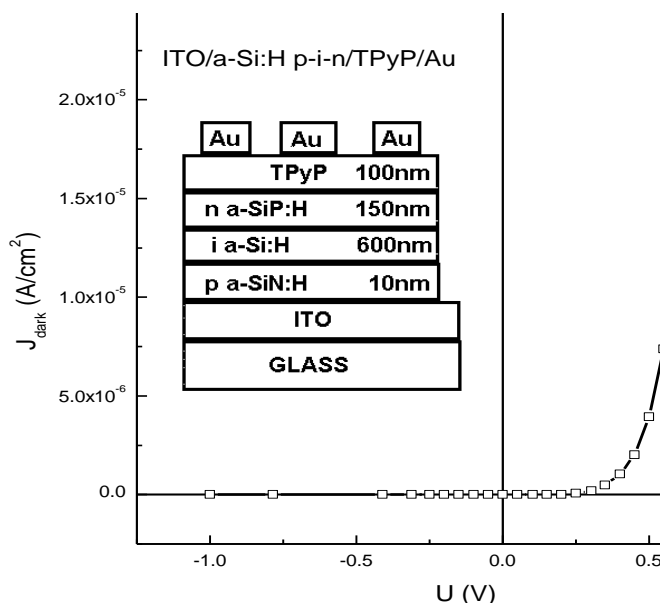


Fig. 15 Cell configuration (inset) and current-voltage characteristics of ITO/a-Si:H p-i-n/TPyP/Au cell. Reprinted with permission from Ref. [48] S. Antohe, L. Ion, N. TomozeiuT. Stoica, E. Barna, *Solar Energy Materials & Solar Cells* **62**, 207 (2000), Copyright Elsevier North-Holland (2000)

The characteristic is asymmetric having very high rectification ratio ( $R_r = 10^4$  at 0.6 V). The behavior of the mentioned structure is due to the energy barrier at the p-i interface, both ITO and Au electrodes giving ohmic contacts with the semiconductor layers, and at the interface a-Si:H/TPyP there is no energy barrier (a-Si:H and TPyP have about the same work functions). The parameters  $n$  and  $I_0$ , having the values: 2.6 and  $1.14 \times 10^{-10}$  A, respectively, have been calculated by the same procedure, used in the case of previous structures. Summarizing, the analysis of the dark current-voltage characteristics was suggested that the ITO/a-Si:H p-i-n/TPyP/Au cell can be considered as p-i-n junction combined with  $R_s$  (which is mainly due to the organic layer).

Fig.16 shows the action spectra of the short-circuit photocurrent for both ITO/a-Si:H p-i-n/Au (a) and ITO/a-Si:H p-i-n/TPyP/Au (b) structures respectively, as well as the absorption spectrum (c) of the TPyP layer.

A marked feature to be noted in Fig.33 curve (b), is that the presence of the TPyP film gives rise to a shift of the long-wavelength edge of the action spectrum of approximately 30 nm to longer wavelengths. The maximum of photocurrent from 500 nm of no sensitised cell is shifted to 530 nm in the case of the sensitized cell. Looking the absorption spectrum of the TPyP layer Fig.33, (c), we can see that the main absorption peaks from 430 nm, 520 nm, 620 nm, are reflected in the action spectrum of the sensitized cell (curve (b)). The area of curve (b) is also larger than that of curve (a). These observations suggest that the sensitization involves an increase of the number of the charge carriers within the a-Si: H p-i-n cell, due to organic layer. Because TPyP is a n-type semiconductor [16], the charge displacement within the cell arises from supplemental injection of electrons from the sensitizing layer.

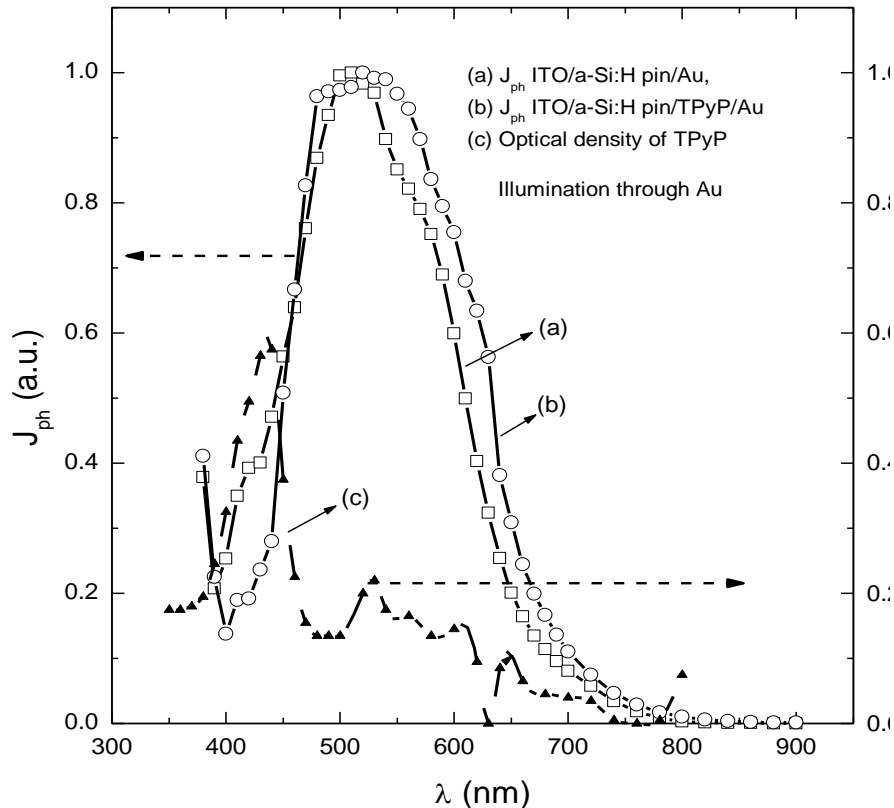


Fig. 16. The action spectra of short-circuit photocurrent of: (a) ITO/a-Si:H p-i-n/Au and (b) ITO/a-Si:H p-i-n/TPyP/Au cells. (c) Optical absorption spectrum of TPyP layer. Reprinted with permission from Ref. [48] S. Antohe, L. Ion, N. Tomozeiu, T. Stoica, E. Barna, *Solar Energy Materials & Solar Cells* **62**, 207 (2000), Copyright Elsevier North-Holland (2000)

The general mechanism of spectral sensitization is: the absorption of the photons in the TPyP creates excitons which diffuse to TPyP/a-Si: H interface, where they dissociate to create free electron-hole pairs. The electrons are injected into TPyP and the holes are displaced by the internal electric field to p-type layer of a-Si: H.

### 3.5 Hybrid inorganic/organic structures

#### 3.5.1 ITO/ZnO/CuPc/Cu

The field of hybrid inorganic/organic heterostructures for photovoltaic applications has attracted much interest in the scientific literature in the last few years. In such structures an organic film is used as absorber, usually in combination with a large band-gap inorganic semiconductor. It is hoped that this combination could result in an increased charge collection by engineering the surface of the inorganic film at nanoscale. The challenge is to create a rough interface between the organic and inorganic layers, with features having dimensions at the scale of diffusion lengths of excitons in the organic material.

Nanostructured ZnO thin films (200 nm thick) were first deposited on 30 nm ITO covered optical glass by PLD (Pulsed Laser Deposition). Then a CuPc film, 600 nm thick, was vacuum sublimated at 400 °C ( $10^{-3}$  Pa residual pressure, 90 °C substrate temperature). Finally, a copper back-contact, 100 nm thick, was vacuum sublimated on top of the structure (Fig. 17a). Action spectrum of the short-circuit current of such a structure is shown in figure 17b, together with the optical absorption spectrum of CuPc layer. It can be easily seen that the features in the action spectrum of the short-circuit current follow closely the ones present in the absorption spectrum of the organic film.

Figure 18 shows the I-U characteristics, recorded in dark and under illumination with monochromatic light, at the wavelength corresponding to the maximum in the action spectrum of the short-circuit current. These are preliminary results, much work is yet to be done to optimize the structure.

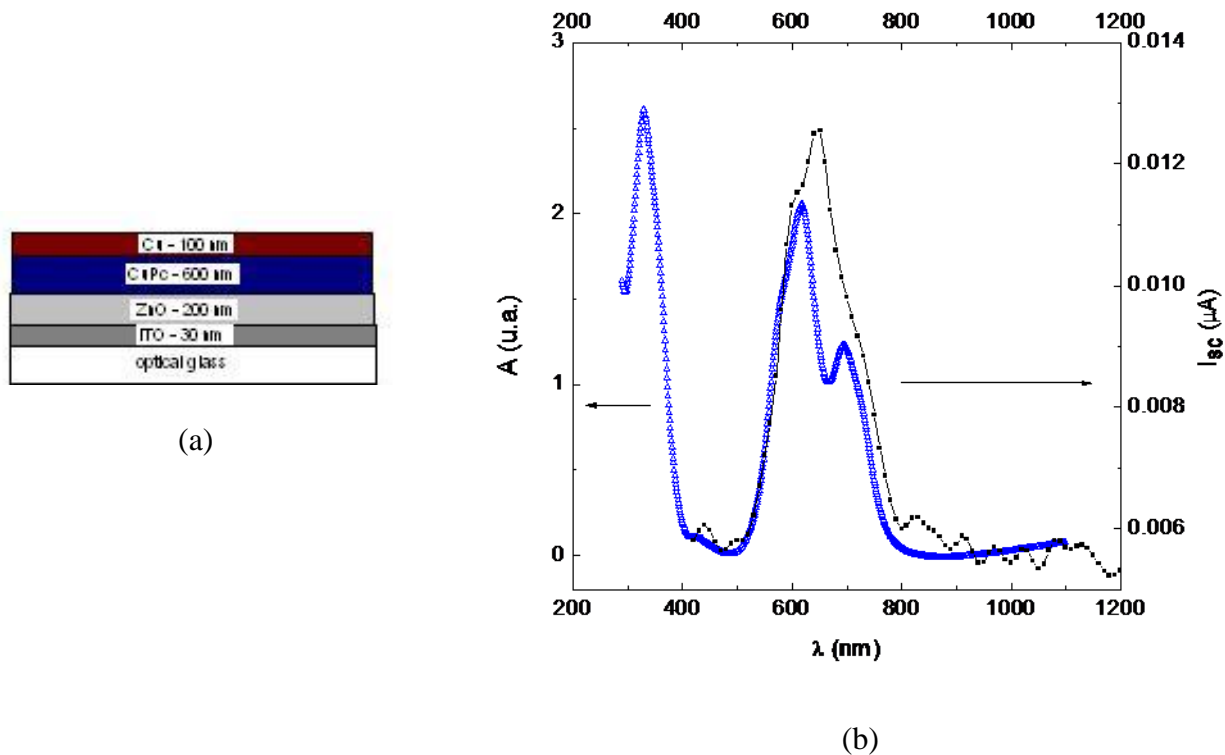


Fig. 17 Configuration of ITO/ZnO/CuPc/Cu cell (a) and absorption spectrum of CuPc film (up-triangles) and action spectrum of short-circuit photocurrent (filled squares) (b).

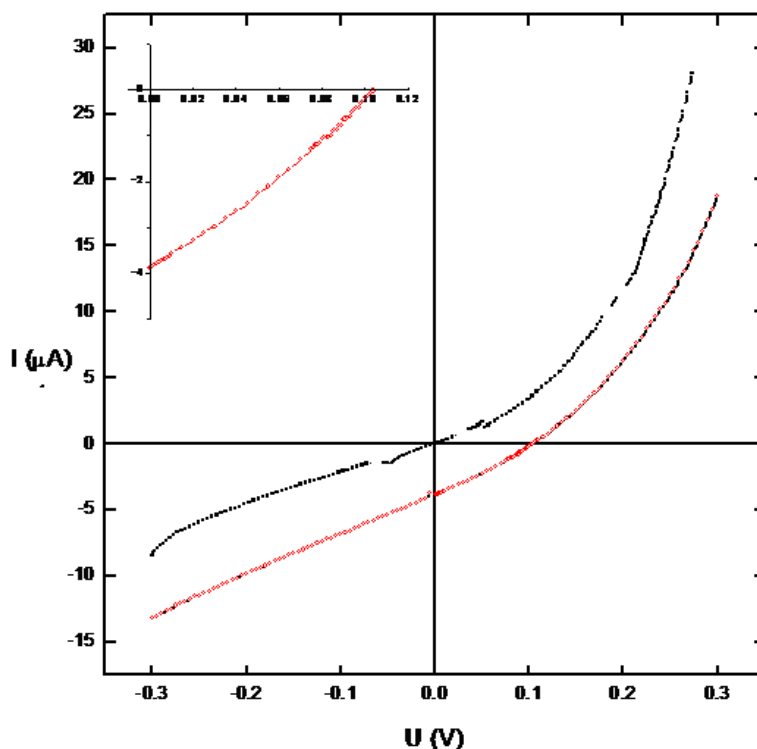


Fig. 18 I-U characteristics of ITO/ZnO/CuPc/Cu cell, recorded in dark (black curve) and under illumination with monochromatic light (660 nm)[76]

### 3. 5. 2 Hybrid CdTe wire arrays/organic dye photovoltaic structures

In the same idea like above presented hybride PV structure, namely that to create a rough interface between the organic and inorganic layers, with features having dimensions at the scale of diffusion lengths of excitons in the organic material, we present here summary, the results obtained from the study on CdTe NW's/Organic Dyes structures.

After establishing the influence of growth conditions on the composition and structure of CdTe wire arrays [77], samples were produced for use in the fabrication of hybrid inorganic/organic photovoltaic structures. A thin film of organic dyes, in our case, either zinc phthalocyanine (ZnPc) or 5,10,15,20-tetrakis(4-pyridyl)-21H,23H-porphine (TPyP), is used as light absorber in such structures [78].

As compared to “classical”, state-of-the-art inorganic solar cells, this type of photovoltaic structures still exhibit rather modest efficiencies. This is essentially due to charge harvesting problems. An excitonic mechanism is responsible for the absorption of the photons in the incident light flux. The problem is that, in spite of the efficiency of the exciton creation process, most of these excitons disappear by direct recombination of the electron-hole pair before reaching an interface where the charge separation can occur.

A better efficiency of exciton dissociation process is expected by creating a large area interface between the organic dye and a nanostructured inorganic semiconductor.

Figure 19 summarizes technological steps in producing hybrid CdTe wire array/organic dye photovoltaic structures.

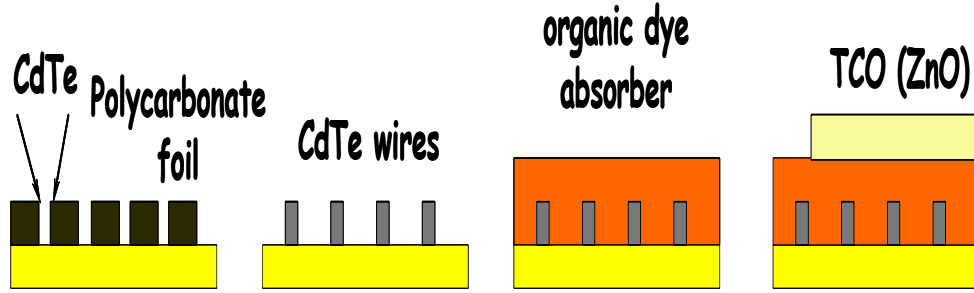


Fig. 19 Technological steps in producing hybrid CdTe wire array/organic dye photovoltaic structures.

After exposing the wire arrays by dissolving the polycarbonate template, an organic dye thin film (400 nm thick) was deposited by thermal evaporation. Then, on top of it, a transparent electrode was grown by pulsed electron deposition. Efforts were made to improve the crystalline quality of the organic dye thin films, because that results in larger exciton diffusion lengths. X-ray diffraction (XRD) pattern obtained for the ZnPc thin film is shown in figure 20a. A Bruker D8 Thin Film high resolution diffractometer was used for structural investigation. A detector scan method, with incident X-ray beam at  $2^\circ$  incidence angle for maximizing the scattering cross-section of X-photons, has been chosen.

The film shows a good crystalline structure. It consist of a monoclinic  $\beta$ -polymorph of ZnPc, highly textured: only (100) peak at  $2\theta=6.9866$  can be observed. The packing b-axis of ZnPc molecules is parallel to the substrate.

An interesting feature can be observed in the X-ray reflectivity pattern of the same film, shown in figure 20b. Kiessig fringes corresponding to a  $156.7 \text{ \AA}$  thick layer can be observed at small angles, near the total reflection critical angle. This layer is probably located at the interface with the substrate.

The spectral dependence of the external quantum efficiency (EQE) of two photovoltaic structures, CdTe nanowires/ZnPc and, respectively CdTe nanowires/TPyP measured at ambient temperature ( $25^\circ\text{C}$ ) is shown in figure 21.

EQE is a characteristic quantity of a photovoltaic structure, measuring the fraction of incident photons for an electron-hole pair collected at its electrodes, in short-circuit condition. It does not consider reflected or transmitted photons.

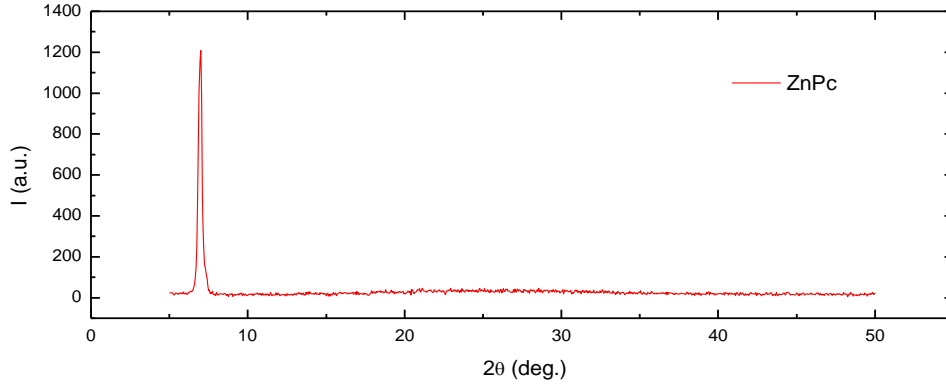
EQE measured under illumination with monochromatic light having the wavelength  $\lambda$ , is given by:

$$EQE(\lambda) = \frac{I_{sc}(\lambda)}{qS\varphi(\lambda)}, \quad (10)$$

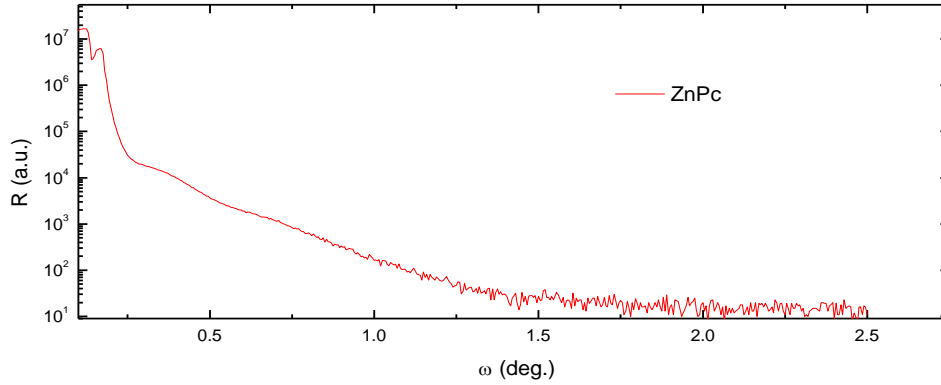
where  $I_{sc}(\lambda)$  is the short-circuit current,  $q$  is the electron charge,  $S$  is the area of the structure and  $\varphi(\lambda)$  is the incident photon flux, given by:

$$\varphi(\lambda) = \frac{P_\lambda}{S \frac{hc}{\lambda}}, \quad (11)$$

$P_\lambda$  being the incident light power,  $h$  Planck's constant and  $c$  light speed in vacuum.



a)



b)

Fig. 20 XRD pattern, recorded in detector scan regime, (a) and omega/2theta specular reflectivity scan (b) of a ZnPc film grown by vacuum thermal evaporation.

Using eqs. (10) and (11), an expression can be obtained, relating EQE to experimentally measurable quantities:

$$EQE(\lambda) = \frac{I_{sc}(\lambda) \cdot hc}{q \lambda P_{\lambda}} \quad (12)$$

In the case of the structure with ZnPc the external quantum efficiency follows the features in the absorption spectra in the investigated spectral region. Those features correspond to Q absorption bands of ZnPc (in the range from 500 nm to 800 nm), associated to  $\pi-\pi^*$  electronic excitations. Under illumination with higher energy photons (low wavelength) EQE increases abruptly, due to B(0,0) and B(0,1) electronic excitations (Soret B band, extending below 400 nm, not shown in the graphs in figure 21). The shoulder at 900 nm is probably due to the onset of light absorption in the CdTe wires.

EQE spectrum recorded in the case of CdTe nanowire array/TPyP exhibits fewer features, especially in the region of Q absorption bands of the porphyrin macrocycle (500 nm to 650 nm) which are “washed” out. The same increase in EQE at the Soret B band (470 nm) can be observed.

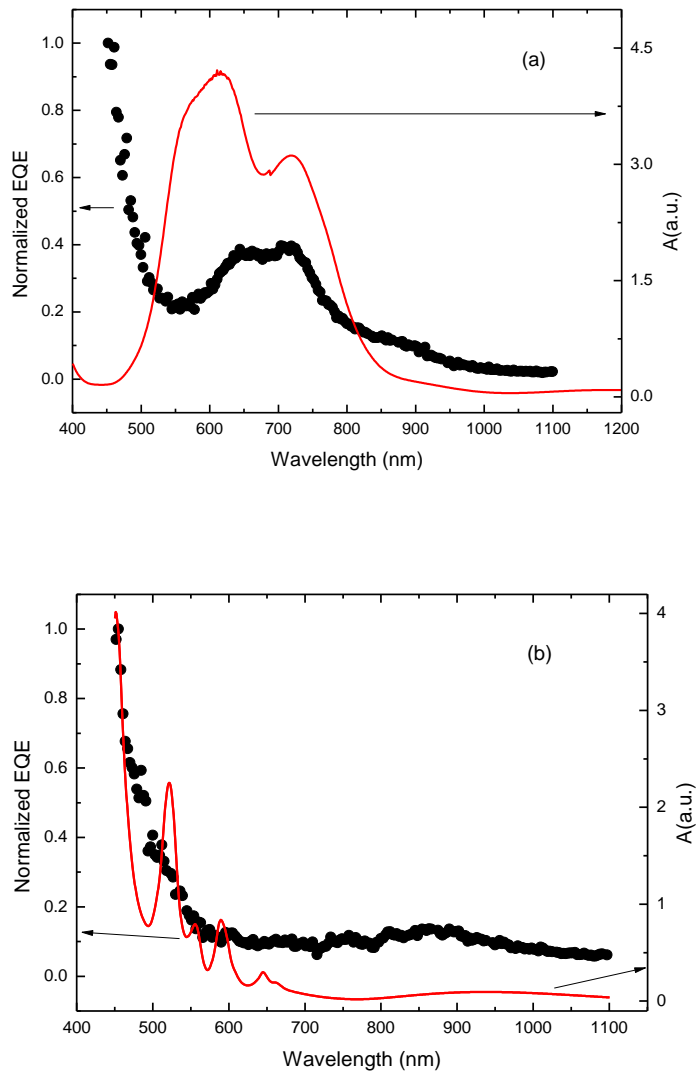


Fig. 21 EQE of a CdTe nanowire array/ZnPc structure (a) and, respectively, of a CdTe nanowire array/TPyP structure (b). For comparison purposes, absorption spectra of ZnPc and TPyP films deposited on optical glass in the same conditions are also given (in red line) [78].

#### 4 Conclusions

- The single - layer ITO/CuPc/Al and ITO/TPyP/Al cells have a photovoltaic response as a result of the charge carrier photogeneration in CuPc or TPyP layer and their separation in the built electric field present at Al/CuPc and ITO/TPyP interface, respectively. The values of the typical cell parameters ( $U_{oc}$ ,  $I_{sc}$ ,  $ff$ , and  $\eta_e$ ) are in good agreement with those of other organic monolayer cells.
- The two-layer ITO/CuPc/TPyP/Al cells have a power conversion efficiency of about 100 times greater than that of organic monolayer cells, due to a strong cosensitization

effect. The ITO/Chla/TPyP/Al cells show rectification and photovoltaic phenomena due to barrier formed at the Chla/TPyP interface. Various photovoltaic features of ITO/Chla/TPyP/Al cells suggest an improvement, although modest, over ITO/Chla/Al cells.

- The three-layered organic photovoltaic cells (ITO/CuPc/(CuPc +TPyP)/TPyP/Al), clearly suggest an improvement, although modest, over two-layered cells. The co deposited interlayer, has been found to act as an efficient carrier photogeneration layer because: on the one hand, the built-in potential drops across it and on the other hand, here there is the region of maximum photogeneration rate, as a result of exciton dissociation via the exciplex of  $(\text{CuPc}^- \dots \text{TPyP}^+)^*$  dyes. The fill factors of 0.11-0.32 represent an improvement over single and double-layered cells. Moreover, the power conversion efficiencies of three-layered cells, ranging from 0.07 to 0.35%, are 2-3 times greater as compared to those for double-layered cells.

- The spectral sensitization of an a-Si:H solar cell using an organic layer was obtained. The action spectrum was extended by 30 nm to longer wavelengths range, using a 100 nm thick layer of TPyP. The sensitization is explained by an exciton dissociation process to the TPyP/a-Si:H interface, which gives rise of higher quantum efficiency at longer wavelengths.

- Hybrid structures like nanostructured ZnO/CuPc/Au or CdTe nw's/ZnPc and CdTe nw's/TPyP, photovoltaic cells showed promising photovoltaic respons, few from them reaching values of the external quantum efficiency more than 12% . However, those structures needs to be improved to increase their optical efficiency and charge collection.

## References

1. A. K. Ghosh and T. Feng, J. Appl. Phys. **49**, 5982 (1978)
2. G. A. Chamberlain, Solar Cells, **8**, 47 (1983)
3. C. J. Brabec, N. S. Sariciftci, and J. C. Hummelen, Adv. Funct. Mater. **11**, 15 (2001)
4. J. Nelson, Organic photovoltaic films, Curr. Opin. Solid State Mater. Sci. **6**, 87 (2002)
5. *Organic Photovoltaics: Concepts and Realization; Springer Series in Materials Science, Vol. 60*, edited by C. J. Brabec, V. Dyakonov, J. Parisi, and N.S. Sariciftci, Springer Verlag, Berlin, (2003)
6. P. Peumans, A. Yakimov, and S.R. Forrest, J. Appl. Phys. **93**, 3693 (2003)
7. S. Antohe and L. Tugulea, phys. stat. sol. (a) **128**, 253 (1991)
8. S. Antohe, I. Munteanu, I. Dima, Rev. Roum. Phys., **34** (6), 665 (1989)
9. S. Antohe, phys. stat. sol. (a) **136**, 401 (1993)
10. T. Stübinger and W. Brütting, J. Appl. Phys. **90**, 3632 (2001)
11. *Primary Photoexcitations in Conjugated Polymers: Molecular Exciton versus Semiconductor Band Model*; edited by N. S. Sariciftci, World Scientific, Singapore (1997)
12. B. A. Gregg and M. C. Hanna, J. Appl. Phys. **93**, 3605 (2003)
13. Fu-Ren, L. R. Faulkner, J. Chem. Phys., **69**, 3334 (1978)
14. K. Yamashita, Y. Matsumura, Y. Harima, S. Miura, and H. Suzuki, Chem. Letters **4**, 489 (1984)

15. S. Antohe, Rev. Roum. Phys., **37**, 309 (1992)
16. F. K. Kampas and M. Gouterman, J. Phys. Chem. **81**, 690 (1977)
17. W. A. Nevin and G. A. Chamberlain, J. Appl. Phys. **69**, 4324 (1991)
18. *Handbook of Organic Conductive Molecules and Polymers; Vol. 1-4*, edited by H.S. Nalwa (John Wiley & Sons Ltd., Chichester, 1997)
19. *Handbook of Conducting Polymers*; edited by T.A. Skotheim, R.L. Elsenbaumer, and J.R. Reynolds (Marcel Dekker, Inc., New York, 1998)
20. *Semiconducting Polymers*; edited by G. Hadziioannou and P.F. van Hutten (WILEY-VCH, Weinheim, 2000)
21. C. W. Tang, Appl. Phys. Lett., **48**, 183 (1986)
22. P. M. Borsenberger, J. Appl. Phys., **62**, 2942 (1987)
23. P. Peumans, V. Bulovic, and S.R. Forrest, Appl. Phys. Lett. **76**, 2650 (2000)
24. J. Xue, S. Uchida, B. P. Rand, and S. R. Forrest, Appl. Phys. Lett. **84**, 3013 (2004)
25. M. Hiramoto, H. Fujiwara and M. Yokoyama, Appl. Phys. Lett., **58**, 1062 (1991)
26. M. Hiramoto, H. Fujiwara, and M. Yokoyama, J. Appl. Phys. **72**, 3781 (1992)
27. S. Antohe, V. Ruxandra. L. Tugulea, V. Gheorghe and D. Ionascu, J. Phys. III France, **6**, 1133 (1996)
28. H. Antoniadis, B. R. Hsieh, M. A. Abkowitz, S. A. Jenekhe, and M. Stolka, Synth. Met. **62**, 265 (1994)
29. N. S. Sariciftci, L. Smilowitz, A. J. Heeger, and F. Wudl, Science **258**, 1474 (1992)
30. L. Smilowitz, N. S. Sariciftci, R. Wu, C. Gettinger, A. J. Heeger, and F. Wudl, Phys. Rev. B **47**, 13835 (1993)
31. C.H. Lee, G. Yu, D. Moses, K. Pakbaz, C. Zhang, N. S. Sariciftci, A. J. Heeger, and F. Wudl, Phys. Rev. B **48**, 15425 (1993)
32. N. S. Sariciftci, D. Braun, C. Zhang, V.I. Srdanov, A. J. Heeger, G. Stucky, and F. Wudl, Appl. Phys. Lett. **62**, 585 (1993)
33. L. S. Roman, W. Mammo, L. A. A. Petterson, M. R. Andersson, and O. Inganäs, Adv. Mater. **10**, 774 (1998)
34. G. Yu, J. Gao, J.C. Hummelen, F. Wudl, and A.J. Heeger, Science **270**, 1789 (1995)
35. C. Y. Yang and A. J. Heeger, Synth. Met. **83**, 85 (1996)
36. J. C. Hummelen, B. W. Knight, F. LePeq, F. Wudl, J. Yao, and C. L. Wilkins, J. Org. Chem. **60**, 532 (1995)
37. G. Yu and A. J. Heeger, J. Appl. Phys. **78**, 4510 (1995)
38. J. J. M. Halls, C. A. Walsh, N. C. Greenham, E. A. Marseglia, R. H. Friend, S. C. Moratti, and A. B. Holmes, Nature **376**, 498 (1995)
39. K. Tada, K. Hosada, M. Hirohata, R. Hidayat, T. Kawai, M. Onoda, M. Teraguchi, T. Masuda, A. A. Zakhidov, and K. Yoshino, Synth. Met. **85**, 1305 (1997)
40. M. Granström, K. Petritsch, A. C. Arias, A. Lux, M. R. Andersson, and R. H. Friend, Nature **395**, 257 (1998)
41. S. E. Shaheen, C. J. Brabec, N. S. Sariciftci, F. Padinger, T. Fromherz, and J.C. Hummelen, Appl. Phys. Lett. **78**, 841 (2001)

42. J. M. Kroon, M. M. Wienk, W. J. H. Verhees, and J. C. Hummelen, *Thin Solid Films* **403-404**, 223 (2002)
43. T. Munters, T. Martens, L. Goris, V. Vrindts, J. Manca, L. Lutsen, W. D. Ceunick, D. Vanderzande, L. D. Schepper, J. Gelan, N. S. Sariciftci, and C. J. Brabec, *Thin Solid Films* **403-404**, 247 (2002)
44. M. M. Wienk, J. M. Kroon, W. J. H. Verhees, J. Knol, J. C. Hummelen, P. A. van Hall, and R. A. J. Janssen, *Angew. Chem. Int. Ed.* **42**, 3371 (2003)
45. W. Geens, T. Aernouts, J. Poortmans, and G. Hadziioannou, *Thin Solid Films* **403-404**, 438 (2002)
46. P. Peumans, S. Uchida, and S.R. Forrest, *Nature* **425**, 158 (2003)
47. D. Gebeyehu, M. Pfeiffer, B. Maennig, J. Drechsel, A. Werner, and K. Leo, *Thin Solid Films* **451-452**, 29 (2004)
48. S. Antohe, L. Ion, N. Tomozeiu, T. Stoica, E. Barna, *Solar Energy Materials&Solar Cells* **62**, 207 (2000)
49. J. Krüger, R. Plass, L. Cevey, M. Piccirelli, M. Grätzel, and U. Bach, *Appl. Phys. Lett.* **79**, 2085 (2001)
50. J. Krüger, R. Plass, M. Grätzel, and H.-J. Matthieu, *Appl. Phys. Lett.* **81**, 367 (2002)
51. W. U. Huynh, J. J. Dittmer, and A. P. Alivisato, *Science* **295**, 2425 (2002)
52. B. O'Regan and M. Grätzel, *Nature* **353**, 737 (1991)
53. K. Kalyanasundaram and M. Grätzel, *Coordin. Chem. Rev.* **77**, 347 (1998)
54. M. Grätzel, *Nature* **414**, 338 (2001)
55. M. Grätzel, *J. Photochem. Photobiol. C* **4**, 145 (2003)
56. U. Bach, D. Lupo, P. Comte, J.E. Moser, F. Weissörtel, J. Salbeck, H. Spreitzer, and M. Grätzel, *Nature* **395**, 583 (1998)
57. D. Gebeyehu, C.J. Brabec, F. Padinger, T. Fromherz, S. Spiekermann, N. Vlachopoulos, F. Kienberger, H. Schindler, and N.S. Sariciftci, *Synth. Met.* **121**, 1549 (2001)
58. Y. Saito, T. Kitamura, Y. Wada, and S. Yanagida, *Synth. Met.* **131**, 185 (2002)
59. E. Arici, N. S. Sariciftci, and D. Meissner, *Adv. Funct. Mater.* **13**, 1 (2003).
60. M. Pientka, V. Dyakonov, D. Meissner, A. Rogach, D. Talapin, H. Weller, L. Lutsen, and D. Vanderzande, *Nanotechnology* **15**, 163 (2004)
61. E. Arici, H. Hoppe, F. Schöffler, D. Meissner, M.A. Malik, and N.S. Sariciftci, *Thin Solid Films* **451-452**, 612 (2004)
62. E. Arici, N. S. Sariciftci, and D. Meissner, in *Encyclopedia of Nanoscience and Nanotechnology*, edited by H. S. Nalwa (American Scientific Publishers, Stevenson Ranch, 2004), Vol.3, pp. 929-944
63. S. Antohe, L. Tugulea, V. Gheorghie, V. Ruxandra, I. Caplanusi and L. Ion, *Phys. Stat. Sol. (a)* **153**, 581 (1996)
64. L. Tugulea and S. Antohe, *Photosynthesis Research II*, 845 (1993)
65. P. Mark and W. Helfrich, *J. Appl. Phys.*, **33**, 205 (1962).
66. H. Meier, *Organic Semiconductors*, (Verlag Chemie, Weinheim 1974)
67. S. Antohe, *Journal of Optoelectronics and Advanced Materials*, **2**, 498 (2000)
68. S. Antohe, *Romanian Reports in Physics*, **53**, 427 (2001)
69. A. Queriagli, H. Kassi, S. Hotchandani and R. M. Leblanc, *J. Appl. Phys.* **77**, 5523 (1992)

70. S. Antohe, D. Ionascu, V. Ruxandra, L. Tugulea, I. Spânulescu, N. Tomozeiu and I. A. Qazii, *Romanian Reports in Physics*, **48**, 581 (1996)
71. Y. Hamakawa, *J.Non-Cryst.Solids*, **59/60**, 1265 (1983)
72. D.E. Carlson, *Sol.Energy Mater.* **3** , 503 (1980)
73. A. M. Barnett and A. Rothwarf, *IEEE Transactions on Electron Devices*, **27**, 615 (1980)
74. A. Matsuda, M. Koyama, Y. Inramishi and K. Tanaka, *Jpn. J. Appl. Phys.* **25**, L54 (1986)
75. A. Morimoto, K. Katoka and T. Shimizu, *Jpn. J. Appl. Phys.* **24**, 1122 (1985)
76. S. Antohe, L. Ion, C. Tazlaoanu, G. Socol, L. Magherusan, I. Enculescu, D. Bazavan, I.N. Mihailescu, and V.A. Antohe, *MRS Spring Meeting 2007, SUA, Symp. Z 4.9*, pg. 538
77. L. Ion, I. Enculescu, Rosemary Bazavan, R. Neuman and S. Antohe, *IMRC, Chongqing, China, June 9-12 2008, Symposium D, O-D11.14*, Pg.173
78. L. Ion, I. Enculescu, Elena Matei, C. Tazlaoanu and S. Antohe, *IMRC, Chongqing, China, June 9-12 2008, Symposium B, P-B3.40*, Pg.55